약학박사학위논문

The oncogenic potential of Nrf2 in diethylnitrosamine-induced murine hepatocarcinogenesis

Diethylnitrosamine 으로 유도된 간암 발생과정 에서 Nrf2의 역할

2017년 8월

서울대학교 대학원
약학과 의약생명과학전공

NGO HOANG KIEU CHI

The oncogenic potential of Nrf2 in diethylnitrosamine-induced murine hepatocarcinogenesis

Diethylnitrosamine 으로 유도된 간암 발생과정 에서 Nrf2의 역할

지도교수 서영준

이 논문을 약학박사 학위논문으로 제출함

2017 년 8 월

서울대학교 대학원

약학과 의약생명과학전공

NGO HOANG KIEU CHI

NGO HOANG KIEU CHI 의 약학박사학위논문을 인준함

2017 년 8 월

위 원 장 _____ (인)

부위원장 _____ (인)

위 원 _____ (인)

위 원 _____ (인)

위 원 _____ (인)

The oncogenic potential of Nrf2 in diethylnitrosamine-induced murine hepatocarcinogenesis

by

HOANG KIEU CHI NGO

A dissertation submitted to the College of Pharmacy in partial fulfillment of the requirements for the degree of

DOCTOR OF PHYLOSOPHY

(Major: Pharmaceutical Bioscience)

Seoul National University

Seoul, South Korea

August, 2017

APPROVED**:**

Advisory Committee Chair, Professor Jung Weon Lee

Advisory Committee Vice-Chair, Professor Marc Francois Diederich

---

Advisory Committee, Professor Kyu-Won Kim

Advisory Committee, Professor Hye-Kyung Na

Advisory Committee, Professor Young-Joon Surh

ABSTRACT

The oncogenic potential of Nrf2 in diethylnitrosamine-induced murine hepatocarcinogenesis

Ngo Hoang Kieu Chi

Under the supervision of professor Young-Joon Surh

Division of Pharmaceutical Bioscience

College of Pharmacy

The Graduate School

Seoul National University

Hepatocellular carcinoma (HCC) is one of the leading causes of cancer-related deaths, and is phenotypically and genetically heterogeneous. Nuclear factor-erythroid 2-related factor 2 (Nrf2, also known as Nfe2l2) is a transcription factor that regulates the expression of a battery of genes encoding phase II carcinogen detoxifying enzymes and

other cytoprotective proteins, hence being considered a prominent target for liver cancer chemoprevention. However, here I unexpectedly found that *Nrf2* knockout mice resisted diethylnitrosamine (DEN)-induced hepatocarcinogenesis without impairment in either metabolic activation of DEN by cytochrome P450 2E1 (Cyp2e1) or hepatic vasculature. In the liver tumors, there was enhanced expression, nuclear translocation, and transcriptional activity of Nrf2. The overactivated Nrf2 was noticed to be required for hepatoma growth during DEN-induced murine HCC. Following DEN treatment, genetic disruption of Nrf2 led to a decrease in the expression levels of a transporter involved in glucose uptake and pentose phosphate pathway (PPP)-related enzymes, whose depletion is reportedly associated with amelioration of HCC. Of note, alterations in the domain binding to its endogenous inhibitor Kelch-like ECH-associated protein 1 (Keap1) likely accounted for the enhanced activity of Nrf2. Additionally, HCC patients bearing activating mutations in *Nrf2* had shorter overall survival compared with their cohort. These findings suggest that Nrf2 is a bona fide liver cancer driver and could serve as a therapeutic target for HCC treatment.

Keywords: Nrf2, diethylnitrosamine, hepatocarcinogenesis, antioxidant response elements, pentose phosphate pathway.

Student Number: 2013-31345

TABLE OF CONTENTS

LIST OF FIGURES

LIST OF ABBREVIATIONS

Nrf2	;	Nuclear factor-erythroid2- related factor 2
WT	;	Wild-type
KO	;	Knockout
ARE	;	Antioxidant responsive element
Ctrl	;	Control
ROS	;	Reactive oxygen species
ECH	;	Erythroid cell-derived protein with CNC homology
Neh	;	Nrf2-ECH-homology
H&E	;	Hematoxylin and eosin
hPAP	;	Human placental alkaline phosphatase
PBS	;	Phosphate-buffered saline
hPAP	;	Human placental alkaline phosphatase
PBS	;	Phosphate-buffered saline
NBT	;	nitroblue tetrazolium
RT-qPCR	;	reverse transcription-quantitative polymerase chain reaction
Cyp2e1	;	Cytochrome P450 2E1
GAPDH	;	Glyceraldehyde-3-phosphate dehydrogenase
PPP	;	Pentose phosphate pathway
Pgd	;	Phosphogluconate dehydrogenase
Me1	;	Malic enzyme 1
G6pd	;	Glucose-6-phosphate dehydrogenase
Tkt	;	Transketolase
Mthfd2	;	Methylenetetrahydrofolate dehydrogenase 2

IDH1	;	Isocitrate dehydrogenase 1
Taldo1	;	Transaldolase 1
PPAT	;	Phosphoribosyl pyrophosphate amidotransferase
PCNA	;	Proliferating cell nuclear antigen
siRNA	;	small interfering RNA
BCIP	;	5-bromo-4-chloro-3-indolyl phosphate, toluidinnium
BrdU	;	5-Bromo-2′-deoxyuridin
DEN	;	Diethylnitrosamine
HCC	;	Hepatocellular carcinoma

INTRODUCTION

1. Keap1/Nrf2/ARE axis

Environmental carcinogens are normally inert chemically and lack ability to modify DNA unless they are converted to reactive species by xenobiotic-metabolizing enzymes (1,2). Biologically reactive metabolites of carcinogens are electrophilic, in general, and hence able to interact covalently with DNA. The resulting DNA adduct formation can cause mutations and consequently carcinogenesis (1,2). To prevent such deleterious effects of chemical carcinogens, the cell mounts various defense mechanisms, such as blockade of the formation of reactive intermediates or stimulation of detoxification through conjugation reaction catalyzed by phase II drug-metabolizing enzymes (3). It is important to note that the majority of genes encoding phase II carcinogen detoxifying enzymes and related cytoprotective proteins contain the consensus sequence 5'-TGCTGAG/CTCAT/C-3' named the antioxidant responsive element (4) or electrophile responsive element (EpRE) in their 5'-flanking regions (5,6).

Nrf2 was first characterized as a transcriptional activator that binds to a tandem repeat sequence named NF-E2 sequence (5'-TGCTGAG/CTCAT/C-3'; ref. (7). Subsequently, Itoh et al. recognized

the similarity between the NF-E2 binding sequence and the antioxidant response element sequence which is identified within the regulatory regions of many antioxidant and phase II carcinogen detoxifying enzymes (8). Hence, it has been widely accepted that activating Nrf2 protects cells from the DNA-damaging effects of reactive oxygen species (ROS) and electrophilic metabolites of carcinogens. Moreover, use of Nrf2 activators has been considered a beneficial therapeutic approach in the management of disorders associated with the accumulation of oxidative stress, such as diabetic complications (9), cardiovascular diseases (10), neurodegenerative disorders (11), and cancer (12).

Human Nrf2 protein is composed of 605 amino acids with seven conserved regions named Nrf2-erythroid cell-derived protein with CNC homology (ECH) domains (Neh) (13) which are distributed along the coding region (**Fig. 1A**). The Neh1 domain is located in the C-terminal half of Nrf2 and contains the CNC homology region and a basic-leucin zipper domain, which allows Nrf2 to form a heterodimer complex with small Maf and then bind to the ARE region in target DNAs (13). The small Maf subunit possesses a leucin zipper domain required for homodimer or heterodimer complex formation with other bZip

transcription factors. Maf can recognize Maf recognition element (MARE), which strikingly resembles ARE consensus sequence, but Maf lacks canonical transcriptional activation domains, hence requiring a CNC factor for the activation function of the heterodimers (14). The proximal amino terminal Neh2 domain negatively regulates Nrf2 through binding of its DLG and ETGE motifs to Keap1 (14,15). The Neh3 domain in the C terminus of Nrf2 allows Nrf2 to interact with a chromo-ATPase/helicase DNA binding protein CHD6, which functions as an Nrf2 transcriptional activator (16). Neh4 and Neh5 adjacent to Neh2 cooperatively bind to cAMP responsive element binding protein (CREBP) binding protein (CBP), which plays an essential role as a coactivator of many transcription factors, to attain the maximal transcriptional activity of Nrf2. CBP-interacting motif in Neh5 is conserved among other members in CNC family, whereas, CBP-binding motif in Neh4 is rather new to that of others in the same family (17). Neh6 contains two phosphorylation-dependent destruction motifs (DSGIS and DSAPGS) recognized by beta-transducin repeats-containing proteins (β-TrCP) of Skp-Cullin1-F-box protein (SCF) E3 ubiquitin ligase complex. Phosphorylation of a Ser cluster in DSGIS motif by glycogen synthase kinase-3 beta (GSK-3β) facilitates the

recognition of Nrf2 by β-TrCP and promotes its ubiquination followed by a rapid turnover (18-20). An Neh7 domain through which retinoic X receptor alpha (RXRα) binds to and subsequently suppresses the transcriptional activation of Nrf2 was then identified in 2013 (21). Under a physiological condition, Nrf2 is sequestered in the cytoplasm due to its binding to Keap1. Keap1 contains two canonical protein interaction motifs: a Broad-complex C, Tramtrack, and Bric-a-brac (BTB) and a double glycine repeat (DGR) or Kelch repeat respectively located in the middle and carboxy terminus, typical of *Drosophila* cytoskeleton binding protein Kelch (14). Two additional domains of Keap1 include interventing region (IVR) and C-terminal region (CTR) (22,23) (**Fig. 1B**). Each Keap1 molecule uses a C-terminal Kelch domain (DGR) to interact separately with two Keap1 binding motifs in the Neh2 domain of Nrf2 (15). The BTB domain allows two Nrf2-bound Keap1 molecules to form a homodimer (24), which serves as an adaptor bridging Nrf2 to Cullin3-associated E3 ubiquitin ligase complex (25,26). The binding of Nrf2 to Cul3 anchored by Keap1 promotes ubiquitin conjugation of lysine residues in the Neh2 domain and therefore marking Nrf2 for degradation by 26 S proteasomes (25,26). Due to the constant exposure of mammalian cells to oxidative

stresses, cystine residues, particularly C273 and C288 residues, in IVR domain in Keap1 would undergo oxidation to form intermolecular disulfide bonds (most likely one C273 of one monomer and C288 of the other), thus covalently linking two monomers of Keap1. Such intermolecular disulfide linkage subsequently introduces an increase in the distance between the two DGR domains of two Keap1 molecules, which possibly dislodges the weaker binding between DGR of the Kelch domain and the DLG motif in Nrf2. Consequently, the modified Keap1 is no longer able to sequester newly synthesized Nrf2 (**Fig. 1C**, left), allowing it to translocate into the nucleus and enhance the expression of phase II enzymes for the clearance or inactivation of the ROS or electrophilic species (15,22,23). Alterations in DLG and ETGE motifs of Nrf2 would lessen the binding between Nrf2 and Keap1 (**Fig. 1C**, right).

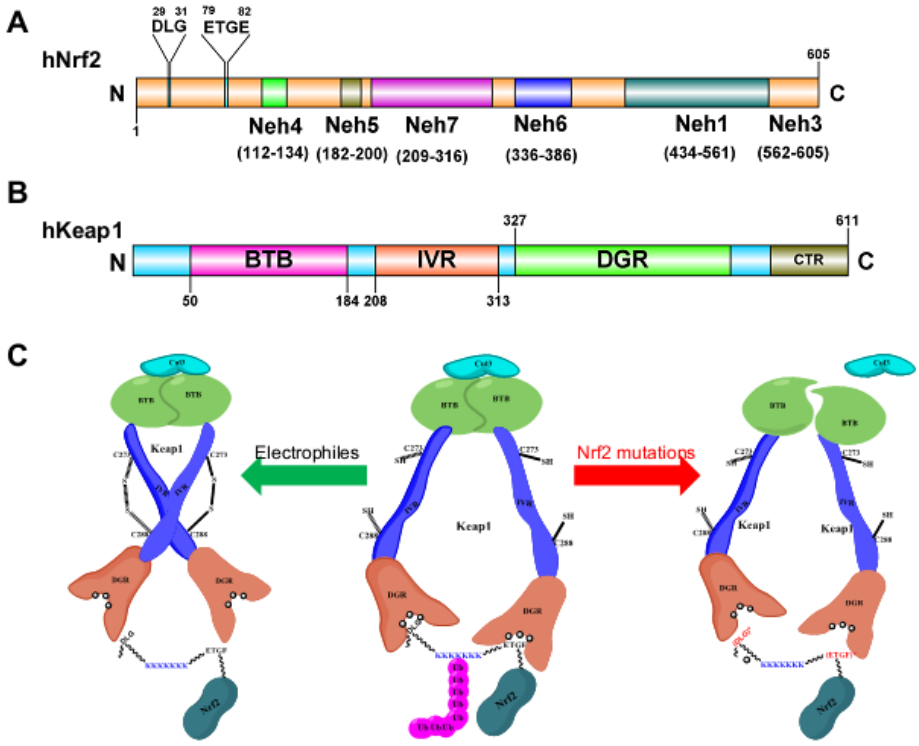
A
hNrf2
29 31 79 82
DLG ETGE
605
N
C
1
Neh4 Neh5 Neh7 Neh6 Neh1 Neh3
(112-134) (182-200) (209-316) (336-386) (434-561) (562-605)
B
hKeap1
327
611
N
BTB
IVR
DGR
CTR
C
50 184 208 313
C
Keap1
Electrophiles
Nrf2 mutations
DGR
Nrf2

Figure 1. **Structures explaining the negative regulation of Nrf2 by Keap1**. (**A**) Structure of Nrf2. The positions of seven Nrf2-ECH homology domains are shown. DLG and ETGE motifs by which Nrf2 associates with Keap1 are highlighted. (**B**) Structure of Keap1. BTB: Broad-complex C, Tramtrack, and Bric-a-brac; IVR: intervening region; DGR: double glycine rich; CTR: Carboxyl terminal region. (**C**) Distortion of Nrf2-Keap1 association. Middle: one Nrf2 molecule use low-affinity DLG and high-affinity ETGF motifs to associate with two Keap1 molecules through its DGR domain. BTB domain in Keap1 allows two Keap1 molecule to form a homodimer and through the same BTB domain recruit Cullin (Cul) 3 to ubiquitinate Nrf2 at lysine residues clustered between DLG and ETGE, finally subjecting Nrf2 to 26S proteasomal degradation. Left: Any genetically changes in either DLG or ETGE motif would lead to the dissociation of Keap1-Nrf2 binding. Right: Disulfide bonds formed due to the reaction of oxidants with reactive thiol groups to cross link two Keap1 molecules, dislodging the attachment of Nrf2 to Keap1.

Paradoxically, cancer cells hijack Nrf2 signaling, and Nrf2 activators turn out to accelerate tumor progression and metastasis in mice (27-29). In this respect, mounting evidence supports that tumors are addicted to Nrf2 signaling (30,31) and some Nrf2-dependent signaling pathways are linked to clinical aggressiveness of cancer cells (31,32). Overexpression/overactivation of Nrf2 frequently observed in various types of cancer is strongly associated with a poor clinical outcome (33,34). Like the majority of other transcription factors, Nrf2 has an inhibitory partner. Thus, Nrf2 forms an inactive complex with Kelch ECH associated protein (Keap) 1 in the cytoplasm (13). Notably, mutations in a region encoding Keap1 binding domain of Nrf2 are commonly observed in cancer, which also contributes to the sustained overactivation of Nrf2 (35).

2. *Nrf2* mutation in cancer

The first study demonstrating the overactivation of Nrf2 in cancer was reported in 2004 by Ikeda et at (36). In the study, mRNA levels of *Nrf2* and placental glutathione S-transferase (*GST-P*), an Nrf2-regulated phase II-detoxifying enzyme that is expressed in cancerous but not normal tissue, were highly elevated in hyperplastic rat liver tissue and

during the course of hepatocellular carcinoma development. The Nrf2-dependent defense response was also found to be activated in various types of cancer including head and neck squamous cell carcinoma (37), and lung cancer (38). Subsequently, it came to be recognized that the Keap1-Nrf2 signaling pathway is largely dysregulated, which would account for the overactivation of Nrf2. Keap1 somatic mutations accompanied by loss of heterozygousity at the gene locus is common in non-small lung cancer, leading to inactivation and consequently the loss of Nrf2 repression by Keap1 (39,40). The reduction of inhibitory effects of Keap1 on Nrf2 activation in cancer could be ascribed to hypermethylation of CpG island in Keap1 promoter in lung cancer tissue and lung cancer cells (41). Moreover, gain-of-function of Nrf2 in cancer commonly arises from genetic alterations in *Nrf2*. Indeed, *Nrf2* is commonly found to be mutated in various types of cancer. The very first study by Shibata et al. uncovered frequent mutations in *Nrf2* in lung cancer cell lines as well as in primary cancer tissue of lung and head and neck cancers (42). *Nrf2* mutations which are mostly of somatic origin were subsequently identified in other types of cancer including oesophageal and skin cancer (43). Data provided by The Cancer Genome Atlas (TCGA) database (http://cancergenome.nih.gov/)

and publicly available at cBioportal (44,45) have uncovered that *Nrf2* mutations are common in primary tumors arising from approximately 20 types of organs (**Fig. 2A**), which have been found to be correlated with its enhanced transcriptional activity (42,43). Among them, lung squamous cell carcinoma carries the highest frequency of *Nrf2* mutation (~19%), followed by head and neck squamous cell carcinoma (~10%) and esophageal adenocarcinoma (~8.5%). Mutations of *Nrf2* are rare in breast, thyroid and brain cancers (**Fig. 2A**). Of note, genetic alterations of *Nrf2* are sorted into DNA amplification and mis-sense mutation with almost the same percentage (**Fig. 2B**). Substitution mutation accounts for most of mis-sense mutation, and substitutions are found all along the coding region of *Nrf2*. It is noticeable that mutations occurring with the highest frequency cluster in either DLG (D29, L30, G31, and R34) or ETGE (E79, T80, G81, and E82) motifs of Neh2 domain (**Fig. 2C**). Genetic alterations in ETGE were experimentally shown to result in the failure in the recognition of Nrf2 by Keap1 regardless of the absence of altered DLG, whereas changes in DLG without alterations in ETGE only affected the binding of DLG with Kelch but not that of wild-type ETGE and Kelch. However, mutations in DLG confer Nrf2 the resistance to ubiquitination, resulting in the

impairment of Keap1-directed proteasomal degradation of Nrf2 (42,46). By contrast, substitutions are rarely found in DNA binding domain of Nrf2 (known as bZIP-Maf or Neh1, **Fig. 2C**), which allows ETGE- or DLG- mutant Nrf2 to maintain its transcriptional activity. Consistently, data from cancer tissues carrying *Nrf2* with aforementioned mutations unveiled that the transcription factor preferentially translocated into the nucleus and were dramatically more active than wild-type Nrf2 (42,43). Note that this represents constitutive activation of Nrf2 in an irreversible. Noticeably, the frequency of substitutions in the Neh6 domain which in addition to the Neh2 domain negatively regulates Nrf2 stability (47) is not distinctive (**Fig. 1C**). Hence, it is likely that cancer cells evolve to have substitutions exclusively clustered in *Nrf2* hotspot regions coding for DLG and ETGE, which allows Nrf2 to bypass the suppression of Keap1, resulting in the overactivation of this transcription factor. The driving mechanism of this phenomenon remains clarified.

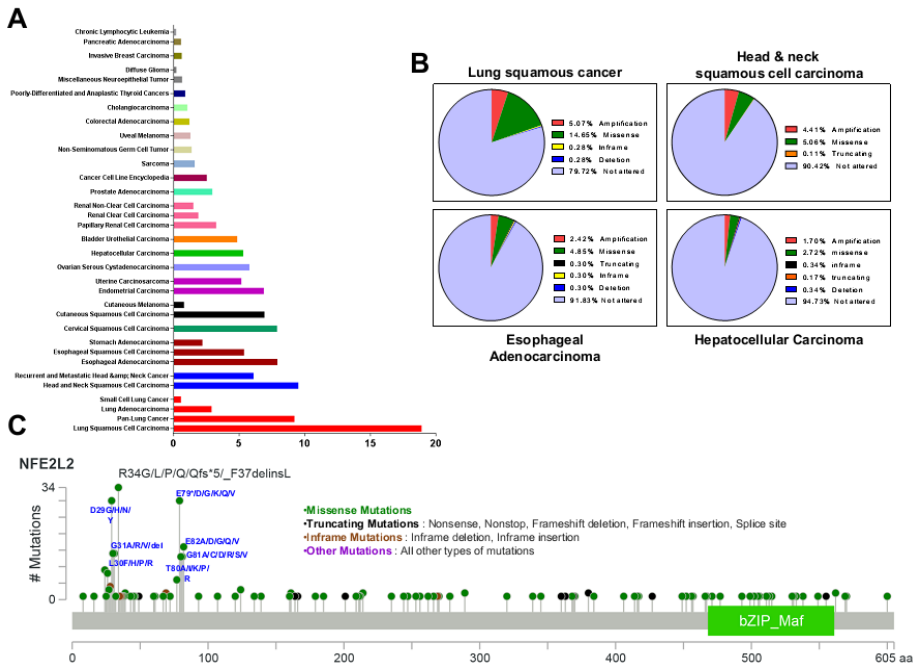

Figure 2. **Nrf2 is frequently mutated in various types of cancer**. (**A**) Frequencies of Nrf2 mutations in many types of cancer. (**B**) Distribution of Nrf2 mutations with amplification and missense mutation occurring at almost the same frequency and accounting for most of Nrf2 genetic alterations. (**C**) Distribution of Nrf2 substitution mutations along the coding region of Nrf2 with the highest frequency clustered in DLG and ETGE motifs.

PURPOSE OF THIS STUDY

Hepatocellular carcinoma (HCC), which comprises approximately 90% of cases of liver malignancy, is the third leading cause of cancer-related mortality worldwide (48) and is associated with diverse etiologic factors, such as hepatitis B and C viral infection, chronic alcohol intake, and exposure to a variety of dietary and environmental chemical carcinogens (49). Recent progress in genomic analyses allows identification of several critical driver mutations and activating signaling pathways involved in HCC development (50,51). Somatic mutations in nuclear factor-erythroid 2-related factor 2 (*Nrf2*, also known as *Nfe2l2*) were also noticed through whole-genome sequencing of HCC patients (48,50). Additionally, somatic mutations in *Nrf2* were noticed as an early molecular event in an experimental model of HCC in rodents (52). However, the biological significance of these changes in the context of Nrf2 involvement in hepatocellular carcinogenesis remained overlooked. Hence in this study, by utilizing *Nrf2* knockout *(*KO) mice in a mouse model of HCC chemically induced by DEN, I aim to investigate the role of Nrf2 in hepatocarcinogenesis and to elucidate the underlying mechanisms.

MATERIALS AND METHODS

1. Animals

Wild-type (WT) and *Nrf2* KO mice on a C57BL6/129SV mixed background generated by the laboratory of Yuet Wai Kan as described previously were used in this study (53). Transgenic (Tg) mice carrying the core ARE sequence coupled to the human placental alkaline phosphatase (hPAP) gene (ARE-hPAP mice) were generously gifted by Dr. Jeffrey A. Johnson (University of Wisconsin-Madison, Madison, WI) (54). In brief, a core sequence ARE carried by 51-bp fragment of rat NAD(P)H:quinone oxidoreductase 1 (Nqo1) was inserted to a TATA-Inr minimal promoter of the heat-stable hPAP reporter construct. This construct was thereafter injected into fertilized oocytes that were then implanted into uteri of surrogate mothers. Resulting pups were identified by genotyping. Mice were maintained in a 12-hour dark-light cycle with the light cycle occurring from 7:00 AM to 19:00 PM and given *ad libitum* access to food and water. All animal experiments were approved by the Seoul National University Animal Care and Use committee (approval number: SNU 20140624-2).

For genotyping, clipped mouse toes were incubated with a genotyping buffer containing 1% sodium dodecyl sulphate (SDS), 0.1

mol/L NaCl, 100 mmol/L EDTA, 50 mmol/L Tris (pH 8.0), and 1 µg/µL proteinase K at 55^0C overnight. On the next day, 5 mmol/L NaCl was added to remove cell debris. DNA was precipitated by incubating in cold 2-propanol at -20^0C for 2 hours, and then washed with cold 70 % ethanol. Six-hundred nanograms of DNA was used as a template for the genotyping PCR following a standard procedure. PCR primer sequences employed are presented in Table 1. Genomic *Nrf2* (g*Nrf2*) was also used as an internal control in genotyping ARE-hPAP mice. PCR products were separated on 2% agarose gels and visualized under imagequant™ LAS 4000 after stained with SYBR®.

2. DEN-induced hepatocellular carcinoma in mice

At day 15 of age, male mice of each genotype (WT and *Nrf2* KO, and ARE-hPAP mice) were given a single dose of 25 mg/kg DEN prepared in PBS (pH 7.4) by intraperitoneal (i.p.) injection, following the protocol described previously (55). Tumor burden was evaluated at indicated times during the course of experiments. Visible nodules (≥ 0.5 mm diameter) were counted (55).

3. Perfusion of the liver with a Trypan blue solution

Perfusion was performed on 15-day-old WT and *Nrf2* KO mice. Mouse liver portal vein was cannulated with a 25-gauge needle connected with a catheter. Subsequently, the inferior vena cava was cut, and the portal vein was perfused with PBS (pH 7.4), followed by a perfusion with a 0.4% solution of trypan blue (Sigma) in PBS.

4. Short-term treatment of animals with DEN

Fifteen-day-old WT and *Nrf2* KO mice were given a dose of 25 mg/kg DEN prepared in PBS (pH 7.4) by i.p. injection. Livers were isolated at indicated times and subjected to subsequent experiments.

5. Hematoxylin and eosin staining

Mice were perfused with PBS (pH 7.4). Livers were isolated, fixed in 4% paraformaldehyde (PFA)/PBS overnight. After paraffin embedding and serial section (5 μm), hematoxylin and eosin (H&E) staining was performed.

6. hPAP staining

Paraffin-embedded tissue sections were deparaffinized by soaking

consecutively in xylene followed by a series of gradient ethanol (100 % x 2 times, 90 %, 80 %, and 70 %) and fixed again in 4% PFA/PBS (pH 7.4), then incubated in PBS at 70 ^{0}C. Slides were thereafter washed in AP buffer (100 mmol/L Tris-HCl pH 9.5, 100 mmol/L NaCl, 50 mmol/L $MgCl_2$, 0.01% sodiumdeoxycholate, and 0.02% Nonidet-P40), and treated with 0.34 mg/ml nitroblue tetrazolium salt (NBT; Sigma) and 0.17 mg/ml 5-bromo-4-chloro-3-indolyl phosphate, toluidinnium salt (BCIP; Sigma) prepared in AP buffer for 18 hours at 37^{0}C. Afterwards, slides were mounted with coverslips, and observed under a light microscope (Leica DM5000B; Leica Microsystems, Inc.).

7. Immunohistological analysis

At the indicated times, mice were perfused with PBS (pH 7.4), and livers were then isolated and fixed in 4% PFA/PBS overnight. After dehydration through a series of gradient sucrose (10% and 30% sucrose in PBS), the livers were immersed in optimal cutting temperature (OCT) embedding compound (Tissue-Tek) and subsequently sectioned at 5 μm thickness on a microtome (HM525; Thermo Scientific). Cryosections were washed briefly with PBS (pH 7.4) and then the nonspecific binding was blocked with a buffer containing 0.3% Triton

X-100 and 5% (v/v) donkey serum (Sigma) in PBS before being incubated with primary antibodies prepared in the blocking buffer at 4^{o}C in a humidified chamber overnight. On the next day, the slides were treated with Alexa 488 and 546 secondary antibodies (Molecular Probe, Invitrogen), followed by nuclear-counterstaining with 4',6-diamidino-2-phenylindole (DAPI; Molecular Probe, Invitrogen). Afterwards, images were obtained under a confocal microscopy (LSM 700; Carl Zeiss).

8. Bromodeoxyuridine staining

Fifteen-day-old WT and *Nrf2* KO mice were given an i.p. dose of DEN (25 mg/kg) prepared in PBS. A single i.p. dose of 50 mg/kg bromodeoxyuridine (BrdU; Sigma) was administered to DEN-injected mice 2 hours before mice were sacrificed. Livers were isolated at 48 hours after DEN injection. Paraffin-embedded liver sections were deparaffinized and subsequently denatured in a mild hydrochloric acid solution before stained with an antibody specific for BrdU. Signals were developed using the ABC staining kit and 3,3’-diaminobenzidine (DAB;Vector Laboratories). The sections were counter-stained with hematoxylin, mounted with coverslips, and visualized under a light

microscope (Leica DM5000B; Leica Microsystems, Inc.).

9. Antibodies

Antibodies used in this study and their sources were glyceraldehyde-3-phosphate dehydrogenase (GAPDH; sc-365062; Santa Cruz; 1:2,000), α-Tubulin (MU-121UC; Biogenex; 1:2,000), β-Actin (A2066; Sigma; 1:2,000), Lamin B (sc-6216; Santa Cruz; 1:2000), Nrf2 (sc-722; Santa Cruz; 1:1000 for Western blotting and 1:200 for immunostaining), Nqo1 (Ab28947; Abcam; 1:2000), cyclin D1 (#2926; Cell Signaling Technology; 1:2000), proliferating cell nuclear antigen (PCNA; #2586; Cell Signaling Technology; 1:500), phosphogluconate dehydrogenase (Pgd; sc-398977; Santa Cruz; 1:2000), malic enzyme (Me) 1 (sc-100569; Santa Cruz; 1:2000), cytochrome P450 2E1 (Cyp2e1; HPA009128; Sigma; 1:1000 for Western blotting and 1:200 for immunostaining), and BrdU (ab1893; Abcam, USA; 1:200).

10. Western blot analysis

Liver tissue was lysed in lysis buffer [50 mmol/L Tris-Cl (pH 7.5), 150 mmol/L NaCl, 1 mmol/L EDTA (pH 8.0), 1% NP-40, 0.25% deoxycholate, protease cocktail tablets]. In some experiments,

hypotonic [10 mM N-2-hydroxyethylpiperazine-N'-2-ethanesulfonic acid (pH 7.9), 1.5 mmol/L MgCl2, 10 mmol/L KCl, 0.5 mmol/L DTT and 0.2 mM PMSF] and hypertonic [20 mmol/L *N*-2-hydroxyethylpiperazine-*N'*-2-ethanesulfonic acid (pH 7.9), 20% glycerol, 420 mmol/L NaCl, 1.5 mmol/L $MgCl_2$, 0.2 mmol/L ethylenediaminetetraacetic acid (EDTA), 0.5 mmol/L DTT and 0.2 mmol/L PMSF] lysis buffers were used for extraction of cytosolic and nuclear proteins. Protein concentrations were measured using Pierce BCA Protein Assay Kit (Thermo Scientific, USA). The lysates were then separated on 8% or 10% SDS-polyacrylamide gels and transferred to polyvinylidene difluoride (PVDF) membranes. Membranes were blotted with different anbitodies and visualized under an imagequant™ LAS 4000 (Fujifilm Life Science, Stamford, USA) for detection of indicated proteins.

11. Reverse transcription-quantitative real-time polymerase chain reaction

Total RNA was isolated from liver tissue using TRIzol® (Invitrogen). RNA was then used to synthesize complementary DNA (cDNA) and further analyzed by quantitative real-time polymerase chain reaction

(qPCR) using RealHelix^{TM} qPCR kit (Nanohelix) with Applied Biosystem 7500 Fast Real-Time PCR System (Applied Biosystem). The relative RNA expression levels were determined accoding to the comparative threshold cycle (Ct value) method. Gapdh was included as an internal control. The primers used in qPCR assay are listed in Table 2.

12. Cell culture and transfection

HEK293T cells were obtained from ATCC in 2010. The cells were cultured in DMEM (Genedepot) supplemented with 10 % v/v FBS and 100 units/mL penicillin and 100 µg/mL streptomycin (Gibco, Invitrogene) in a humidified atmosphere of 95% O_2 and 5% CO_2 in an incubator at 37^0C and used within ten passages. *Mycoplasma* test was routinely performed using a BioMycoX® Mycoplasma PCR Detection Kit (CellSafe) to ensure that cells were negative for *Mycoplasma* contamination. As HEK293T cells are solely used as an expression system but not for cancer-related biological studies, they were not authenticated. The cells were transfected with indicated plasmids using transfection reagent polyethylenimine (PEI; Sigma) following manufacturer's instructions. Twenty-four hours after transfection, the

cells were harvested for subsequent assays.

13. Sequencing

Total RNA was extracted from vehicle- or DEN-treated liver tissue and converted to cDNA using reverse transcriptase enzyme following the standard procedure. The cDNA region bearing exon 2 of murine *Nrf2* gene was amplified using PCR with HiPi Taq polymerase (Elpisbio). The PCR products were purified by QIAquick PCR Purification Kit (Qiagene), and sequenced by ABI PRISM 3130xl Genetic Analyzer (Applied Biosystems). Primers for sequencing are listed in Table 3. Mutations are defined and given in accordance to the numbering of amino acid in murine Nrf2 protein sequence (NCBI CCDS Database; gene number: NC_000068.7)

14. Plasmids and site-directed mutagenesis

A plasmid of pcDNA3.1-EGFP-C4-human *NRF2* was obtained from Addgene (plasmid #21549, generated by Dr. Yue Xiong's lab). For a murine Nrf2 expression vector, a plasmid of murine *Nrf2* (AAV-MCS8-Nrf2) was purchased from Addgene (plasmid #67636, generated by Dr. Connie Cepko's lab). Various constructs of *Nrf2* bearing point

mutations were generated using Muta-Direct Site Directed Mutagenesis Kit (iNtRON). A stop codon ATG was introduced to the murine *Nrf2* construct to halt the expression of Nrf2. Primer sequences used appear in Table 4. All plasmid clones were verified by DNA sequencing.

15. Clinical data collection

The cBioPortal for Cancer Genomics (http://www.cbioportal.org/) (44,45) is the main source of information. In total, data from 231 HCC cases provided by ASAN Medical Center (AMC) (56) and 356 HCC cases obtained from The Cancer Genome Atlas (TCGA) Research Network (http://cancergenome.nih.gov/) were collected and sorted into groups with WT or mutant *Nrf2* before being subjected to Kaplan-Meier survival analysis. Raw data are provided in Dataset 1. The statistical significance of differences between two groups was evaluated based on log-rank test. Data are presented as mean ± SEM. Data analyses were performed using Graphpad Prism (Version 6).

16. Statistical analysis

The statistical significance of differences between two groups was evaluated based on two-tailed Student *t* test. Statistical significance was

accepted at $P < 0.05$. $^{*}P < 0.05$, $^{**}P < 0.01$; $^{***}P < 0.001$; $^{\#}P < 0.0001$. Data are presented as mean ± SEM. Data analyses were performed using Graphpad Prism (Version 6).

RESULTS

Nrf2 deficiency abolishes hepatoma burden in mice treated with DEN

To investigate the role of Nrf2 in liver tumorigenesis, I compared the development of HCC in WT and *Nrf2* KO mice. Their genotype was verified by genotyping (**Fig. 3A**). Male mice of each phenotype were given a single i.p. injection of DEN at day 15 after birth following the protocol described previously (55). After 9 months, I noticed that all the WT mice treated with DEN developed hepatomas, whereas no tumors were visible in the livers of *Nrf2* KO mice with the same treatment (**Fig. 3B**).

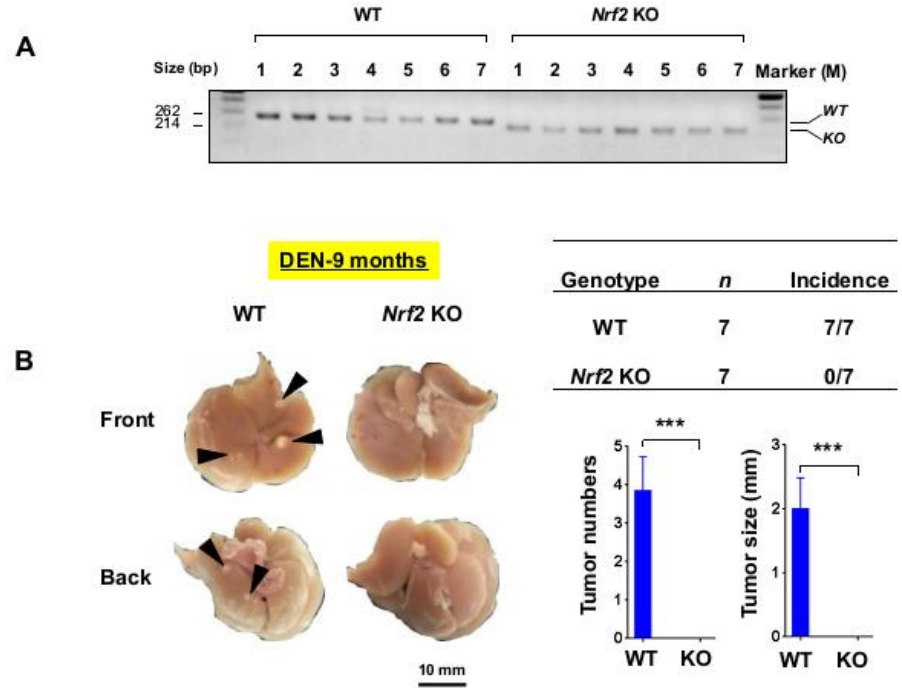

Figure 3. *Nrf2* KO mice are resistant to DEN-induced hepatocarcinogenesis after 9 months of DEN treatment. (**A**) WT and *Nrf2* KO male mice were identified by genotyping. (**B**) Male mice of each genotype (n = 7 mice per genotype) were given DEN at the postnatal day 15 and evaluated for tumor burden at the age of 9 months. Gross morphology of livers, the proportion of liver tumor-bearing mice, the number of tumors per mouse liver (diameter ≥ 0.5 mm), and diameter of individual tumor in livers of WT and *Nrf2* KO mice by the age of 9 months are shown. Arrows indicate tumor nodules. Scale bar, 10 mm (**B**). Data represent mean ± standard error of the mean (SEM), $^{***}P < 0.001$; two-tailed Student t test.

I subsequently examined the liver sections of DEN-treated WT and *Nrf2* KO mice by H&E staining. WT mice showed multiple lesions with normal hepatocytes interspaced among the tumor cells, whilst the livers from *Nrf2* KO mice showed a conserved normal hexagonal structure (**Fig. 4**).

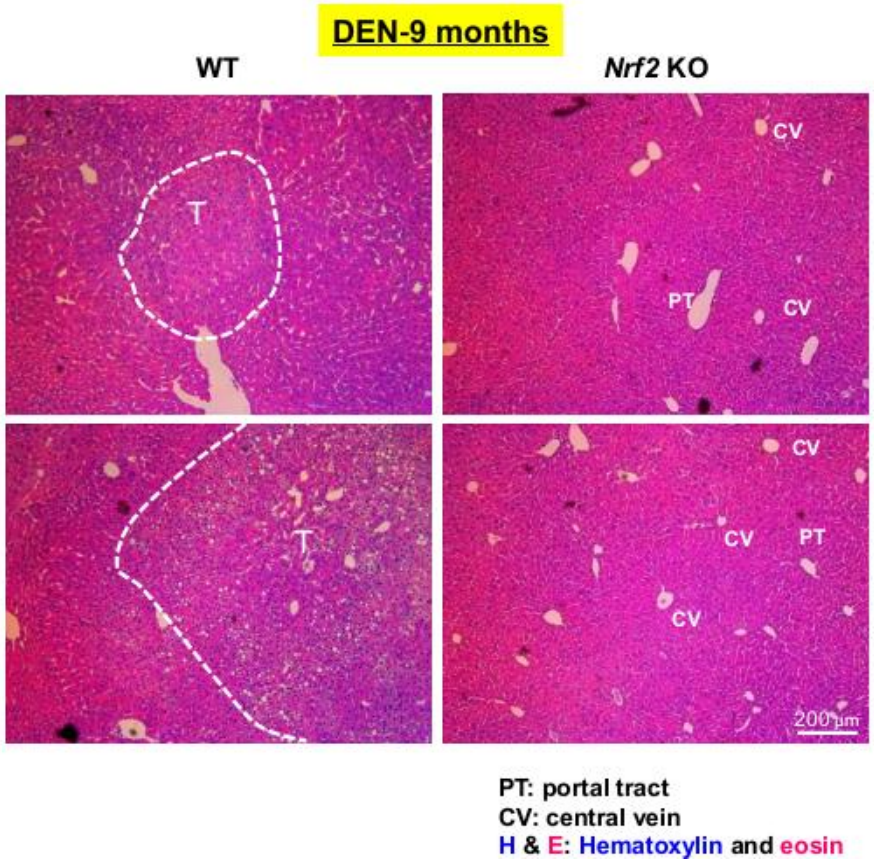

Figure 4. H&E staining of liver sections from WT and *Nrf2* KO mice treated with DEN for 9 months. Fifteen-day-old WT and *Nrf2* KO male mice were given a single i.p. dose of DEN. At the age of 9 months, mice were killed and their liver sections were subjected to H&E staining. Abbreviations: T, tumor; CV, central vein; PT, portal triad. Scale bars, 200 µm.

I further confirmed this result in another set of mouse livers collected at 14 months after the DEN injection, the duration reported to cause an advanced stage of HCC in the DEN-induced HCC mouse model (57). Again, the *Nrf2* KO mice had no visible tumors in livers even at 14 months after the DEN injection, while all of the WT mice showed severe tumor burden (**Fig. 5**).

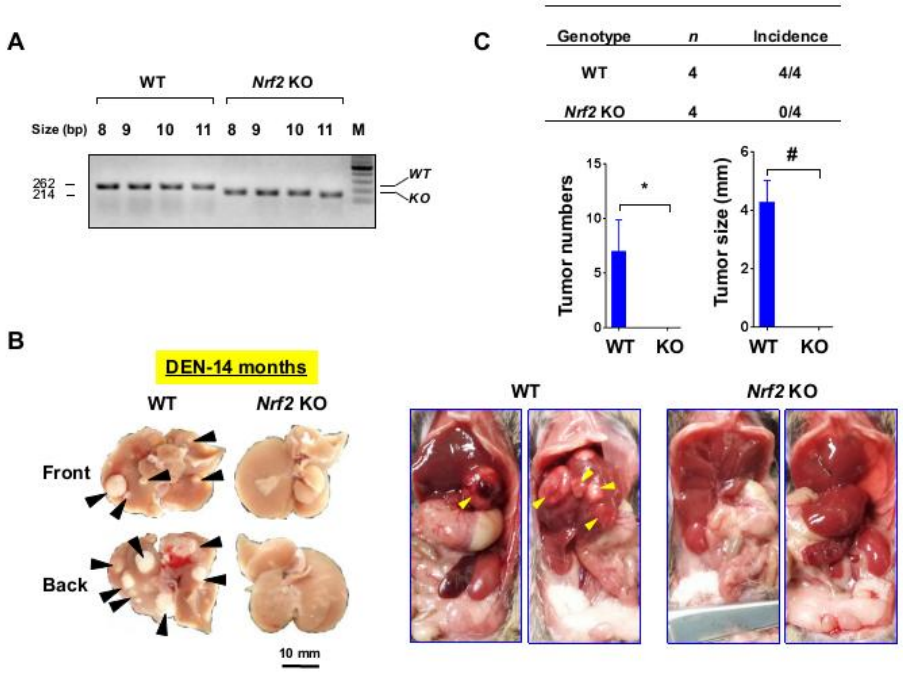

Figure 5. *Nrf2* KO mice are resistant to DEN-induced hepatocarcinogenesis after 14 months of DEN treatment. (**A**) WT and *Nrf2* KO male mice were identified by genotyping. (**B**) Male mice of each genotype (n = 4 mice per genotype) were given DEN at the postnatal day 15 and evaluated for tumor burden at the age 14 months. Gross morphology of livers (**B**), the proportion of liver tumor-bearing mice, the number of tumors per mouse liver (diameter ≥ 0.5 mm), and diameter of individual tumor (**C**) in livers of WT and *Nrf2* KO mice by the age of 14 months are shown. Arrows indicate tumor nodules. Scale bars, 10 mm (**B**, left). Data represent mean ± standard error of the mean

(SEM). $^{*}P < 0.05$, $^{\#}P < 0.0001$; two-tailed Student's *t* test.

H&E staining of DEN-treated liver sections revealed hepatic lesions in the WT mice but a normal hexagonal liver structure in the *Nrf2* KO mice without tumors (**Fig. 6**). Collectively, these results indicate that deletion of *Nrf2* confers resistance to DEN-induced hepatocarcinogenesis in mice.

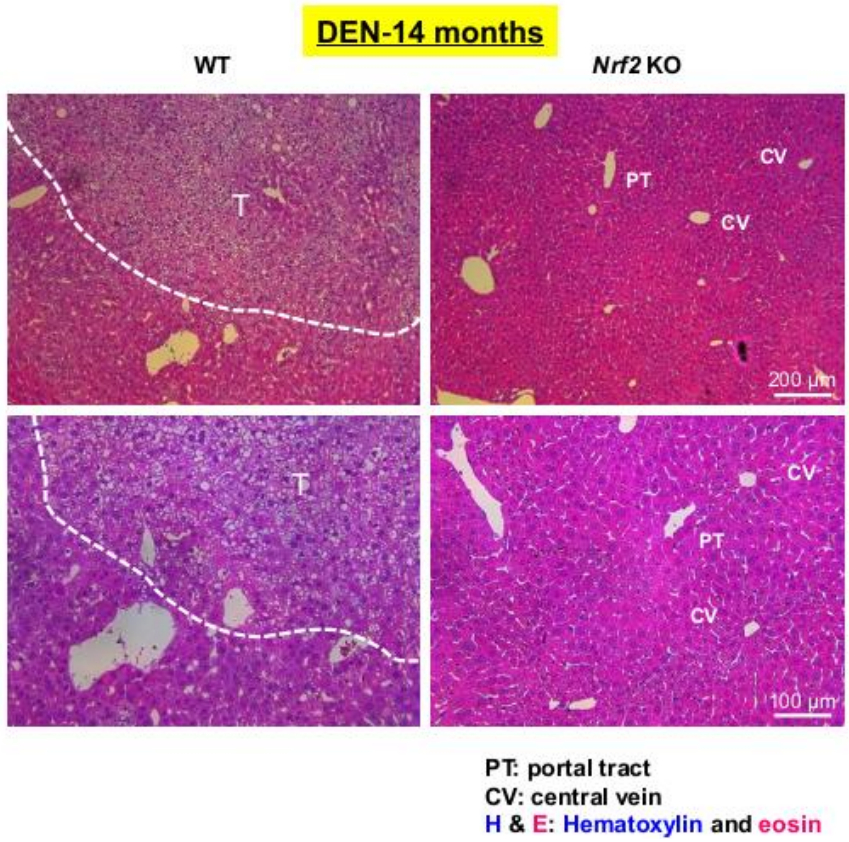

Figure 6. H&E staining of liver sections from WT and *Nrf2* KO mice treated with DEN for 14 months. Fifteen-day-old WT and *Nrf2* KO male mice were given a single i.p. dose of DEN. At the age of 14 months, mice were killed and their liver sections were subjected to H&E staining. Abbreviations: T, tumor; CV, central vein; PT, portal triad. Scale bars, 200 μm (58), and 100 μm (bottom).

Nrf2 KO mice show normal expression of hepatic Cyp2e1 but lowever levels of phase II detoxifying enzymes

DEN undergoes initial metabolic conversion to a reactive α-hydroxydiethylnitrosamine (hydroxylated DEN) by hepatic cytochrome P450 (CYP)-dependent monooxygenases, followed by the formation of an ethyldiazonium ion intermediate that gives rise to DNA-adducts (59). Among CYPs involved in the bioactivation of DEN, cytochrome P450 2E1 (Cyp2e1) has been considered to be the primary catalyst (59,60). Accordingly, I compared the expression levels of Cyp2e1 in 15-day-old WT and *Nrf2* KO mice at 6 and 48 hours after DEN injection. The results show that the hepatic protein levels of Cyp2e1 were not significant different between WT and *Nrf2* KO mice (**Fig. 7**).

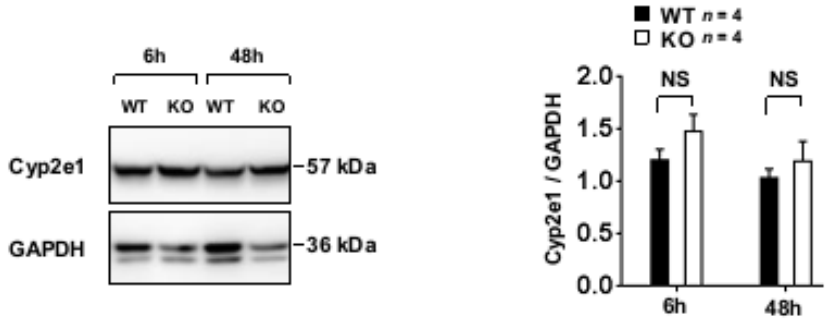

Figure 7. Cyp2e1 expression in *Nrf2* KO mice is comparable to WT mice. Fifteen-day-old mice were intraperitoneally injected with DEN (*n* = 4 mice per genotype) and killed at 6 or 48 hours. Their livers were harvested for subsequent experiments. Hepatic Cyp2e1 expression was measured by Western blot analysis (left), showing the same level of Cyp2e1 expression in the liver of WT and *Nrf2* KO mice. Densitometric quantification of Cyp2e1 is shown (*n* = 4 mice per genotype; right). Error bars show the SEM. NS: non-significant; two-tailed Student's *t* test.

Immunohistological (IHC) analysis also revealed that WT and *Nrf2* KO mice displayed a similar zonation of Cyp2e1 in the centrilobular region of the liver where the distribution of Cyp2e1 is mainly confined (61) (**Fig. 8**).

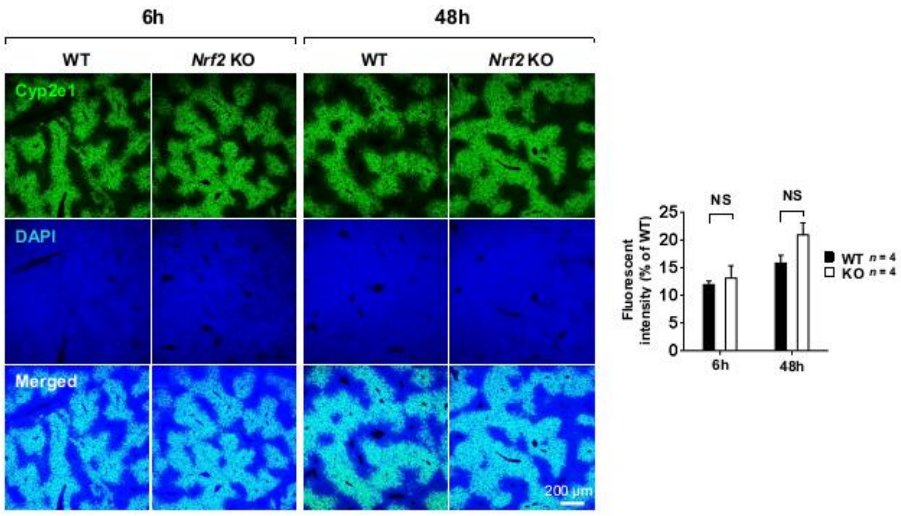

Figure 8. Cyp2e1 expression in *Nrf2* KO mice is comparable to WT mice. Fifteen-day-old mice were intraperitoneally injected with DEN (*n* = 4 mice per genotype) and killed at 6 or 48 hours. Liver sections of both genotypes were immunostained with Cyp2e1 antibody, demonstrating the similar areas of Cyp2e1 expression in the centrilobular zone **(A)**. DAPI was used to label cellular nuclei. Scale bars, 200 µm. (**B**) Quantification of fluorescent intensity of Cyp2e1 staining in (**A**) is shown (*n* = 4 mice per genotype). Error bars show the SEM. NS: non-significant; two-tailed Student *t* test.

In addition, the biotransformation of DEN by CYPs also initiates its detoxification in the liver by phase II enzymes particularly UDG-glucuronosyltransferases (Ugts) as the first derivative α-hydroxydiethylnitrosamine was reported to be prone to glucuronidation, permitting it to be excreted in the urine (62). Examination of hepatic Ugts by qPCR uncovered that the mRNA levels of *Ugt1a1* and *Ugt1a6* after 48 hours of DEN injection at day 15 were higher in WT compared to those in *Nrf2* KO mice (**Fig. 9**), suggesting of an even more effective toxicant elimination process in WT but not mice deficient in *Nrf2*. The observation is not unexpected, for the transcription of *Ugts* is largely regulated by Nrf2 (63,64).

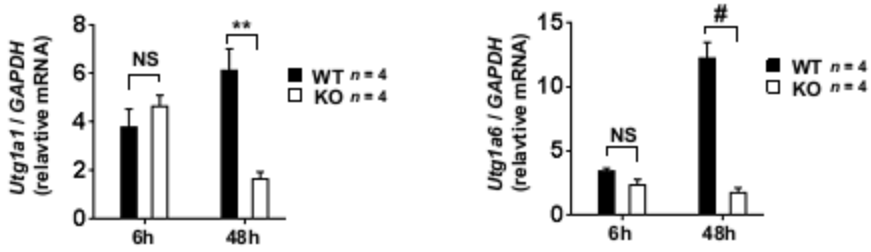

Figure 9. **The mRNA levels of Ugt1 phase II detoxifying enzymes are higher in WT mice than in *Nrf2* KO mice**. Fifteen-day-old mice were intraperitoneally injected with DEN (*n* = 4 mice per genotype) and killed at 6 or 48 hours after the injection. mRNA levels of phase II enzymes Ugt1a1 and Ugt1a6 in the livers were determined by RT-qPCR (n = 4 mice per genotype). Error bars show the SEM. **P < 0.01, #P < 0.0001, NS: non-significant; two-tailed Student *t* test.

***Nrf2* KO mice do not exhibit hepatic vascular anomalies.**

The magnitude of the carcinogenicity of DEN could be determined by its bioavailability in the liver as well, which is in part affected by the degree of blood supply to the hepatocytes. A vascular anomaly, such as portosystemic shunt, would decrease the amount of chemicals carried to the liver (65). To ascertain whether or not any congenital malformations possibly present in the hepatic vasculature of *Nrf2* KO mice I used could affect the delivery of DEN to the liver, I perfused the livers of 15-day-old mice with a 0.4% solution of Trypan blue. The perfusion showed that the Trypan blue perfused, through the hepatic portal vein, penetrated the liver vasculature of *Nrf2* KO mice as well as WT mice (**Fig. 10**).

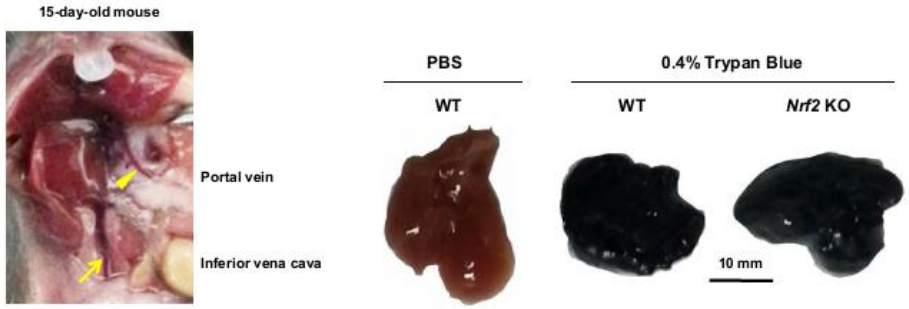

Figure 10. *Nrf2* KO mice do not exhibit hepatic shunt. The livers of 15-day-old mice were perfused with a 0.4% solution of Trypan blue (*n* = 3 mice per genotype). Representative livers following Trypan blue perfusion are shown.

In addition, none of the *Nrf2* KO mice examined displayed dysplasia in the regions surrounding the portal triad (**Fig. 11**). These findings suggest that the genetic disruption of *Nrf2* does not provoke noticeable hepatic vascular abnormalities in the mice used in the current study.

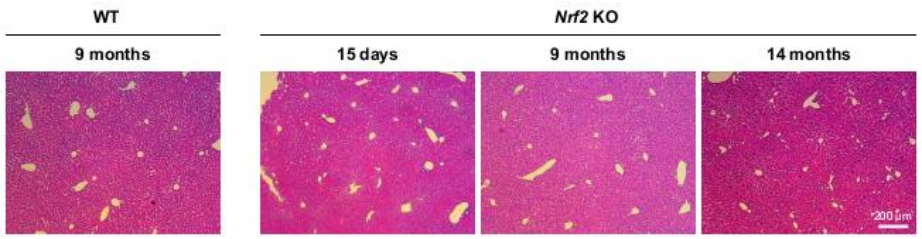

Figure 11. *Nrf2* KO mice do not exhibit hepatic anomalies. Representatives of H&E-stained liver sections from WT aged 9 months, 15-day-old *Nrf2* KO (n = 9 mice), and 9- (n = 7 mice) and 14- (n = 4 mice) month-old mice which were used to compare the tumor burden in response to DEN treatment between genotypes.

Nrf2 is overexpressed and activated in the hepatomas of DEN-treated mice

To understand the mechanisms by which *Nrf2* drives tumor progression in the liver of DEN-treated mice, I first determined the level of Nrf2 expressed in hepatomas. As shown in Figure 12A, Nrf2 was detected at elevated levels within the DEN-induced liver tumors as compared with that in the normal liver tissue of vehicle-treated WT mice. In addition, IHC analysis showed an increase in the levels of Nrf2 in the hepatomas (**Fig. 12B**).

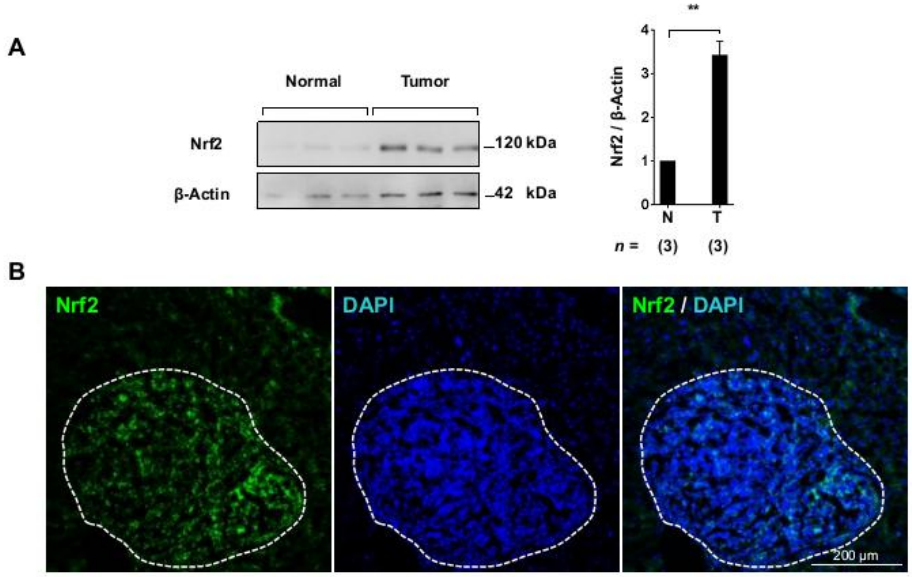

Figure 12. Nrf2 is overexpressed in hepatomas of DEN-treated WT mice. (**A)** Total lysates from either livers of vehicle (PBS)-treated mice or hepatomas of 9-month-old mice given DEN were analyzed by immunoblotting. Results show the overexperssion [**A;** *n* (tissue) = 3 from 3 mice] of Nrf2 in tumors. Western blot analysis of Nrf2 protein levels (left) and the corresponding quantifications are shown (right). β-Actin was used as a loading control. (**B**) Liver sections from DEN-treated WT mice at the age of 9 months were subjected to Nrf2 staining (green). DAPI (dark blue) was used to label cellular nuclei. Data are the representative of three different samples. Scale bars, 200 μm (**B**). Error bars show the SEM. $^{**}P < 0.01$; two-tailed Student's *t* test.

Abbreviations: N, normal; T, tumor.

Furthermore, examining cytosolic and nuclear extracts from livers of vehicle-treated mice or hepatomas of 9-month-old mice given DEN by Western blotting, I noticed that nuclear accumulation of Nrf2 was increased markedly in the tumors (**Fig. 13**).

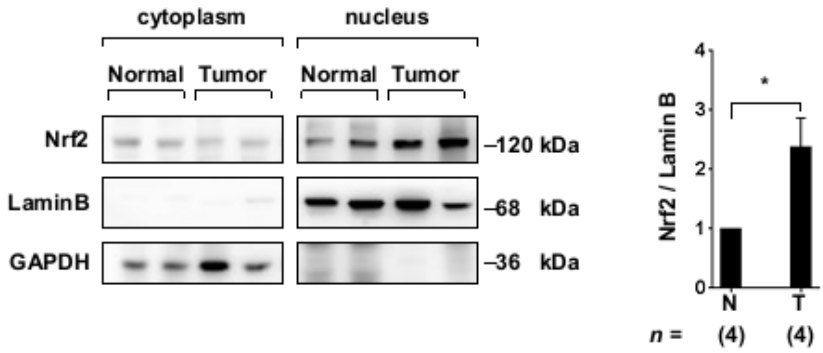

Figure 13. Nuclear translocation of Nrf2 is enhanced in hepatomas of DEN-treated WT mice. Cytosolic and nuclear factions from either livers of vehicle (PBS)-treated mice or hepatomas of 9-month-old mice given DEN were analyzed by immunoblotting [*n* (tissue) = 4 from 4 mice]. Results show the nuclear accumulation of Nrf2 in tumors. Western blot analysis of Nrf2 protein levels (left) and the corresponding quantifications are shown (right). GAPDH and lamin B are cytosolic

and nuclear markers, respectively. Error bars show the SEM. $^{*}P < 0.05$; two-tailed Student's *t* test.

The overexpression and increased accumulation of Nrf2 in the nucleus were found to be functional as indicated by an increased expression of the principal target gene NAD(P)H quinine oxidoreductase 1 (*Nqo1*) (12) at both protein (**Fig. 14A**) and mRNA levels (**Fig. 14B**).

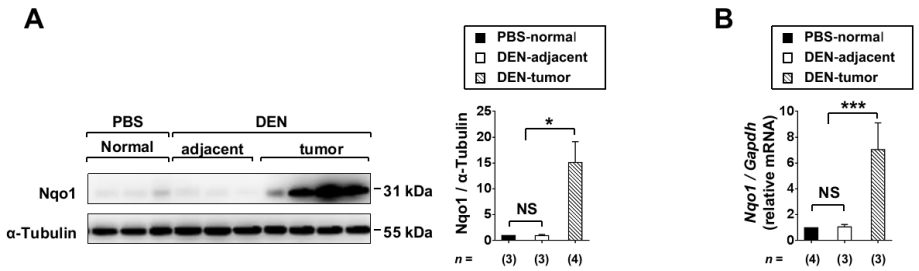

Figure 14. The expression of Nqo1 is enhanced at both protein and mRNA levels in hepatomas. Total mRNA or protein samples were prepared from tumors, non-tumor adjacent tissue, and vehicle (PBS)-treated livers of 9-month-old mice, and subjected to Western blotting with an antibody against Nqo1 [**A**; *n* (tissue) = 3-4 from 3 mice] or RT-qPCR with specific primers for Nqo1 [**D**; *n* (tissue) = 3-4 from 3 mice]. Gapdh and α-Tubulin served as internal controls. Error bars show the SEM. $^{*}P < 0.05$, $^{**}P < 0.01$, $^{***}P < 0.001$, NS: non-significant; two-tailed Student's *t* test.

To more precisely examine the transcriptional activity of Nrf2 in the hepatomas, ARE-hPAP Tg reporter mice were utilized (54). These mice carry a construct of a reporter gene *hPAP* containing a core sequence ARE, which is expressed under the control of Nrf2, hence its expression could specifically represent the transcriptional activity of Nrf2 (**Fig. 15A**). Tumors derived from ARE-hPAP mice given DEN (**Fig. 15B**) were subjected to hPAP staining, a reaction in which two substrates BCIP and NBT are catalyzed by hPAP to blue-purple precipitates which can be visualized under a microscopy.

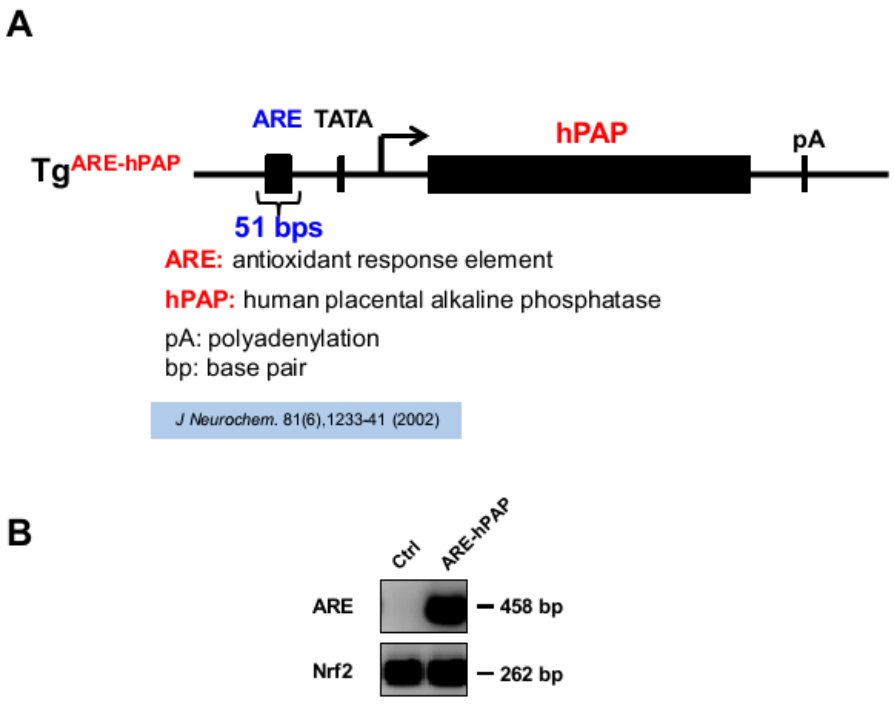

Figure 15. ARE-hPAP mice were used to measure transcriptional activity of Nrf2 *in vivo*. (**A**) Strategy for generation of ARE-hPAP Tg mice (upper). pA, polyA; ARE: a core sequence ARE. TATA: TATA box. hPAP: heat-stable human placental alkaline phosphatase reporter gene construct (upper panel). (**B**) Genotyping of ARE-hPAP mice and their control littermates which had been subjected to DEN injection at the age of 15 days.

Liver sections from DEN-treated ARE-hPAP mice displayed strong hPAP activity in the tumors, reflecting the enhanced transcriptional activation of Nrf2 (**Fig. 16**). Together, these results indicate that Nrf2 is functionally overactivated in the hepatomas of DEN-treated mouse livers.

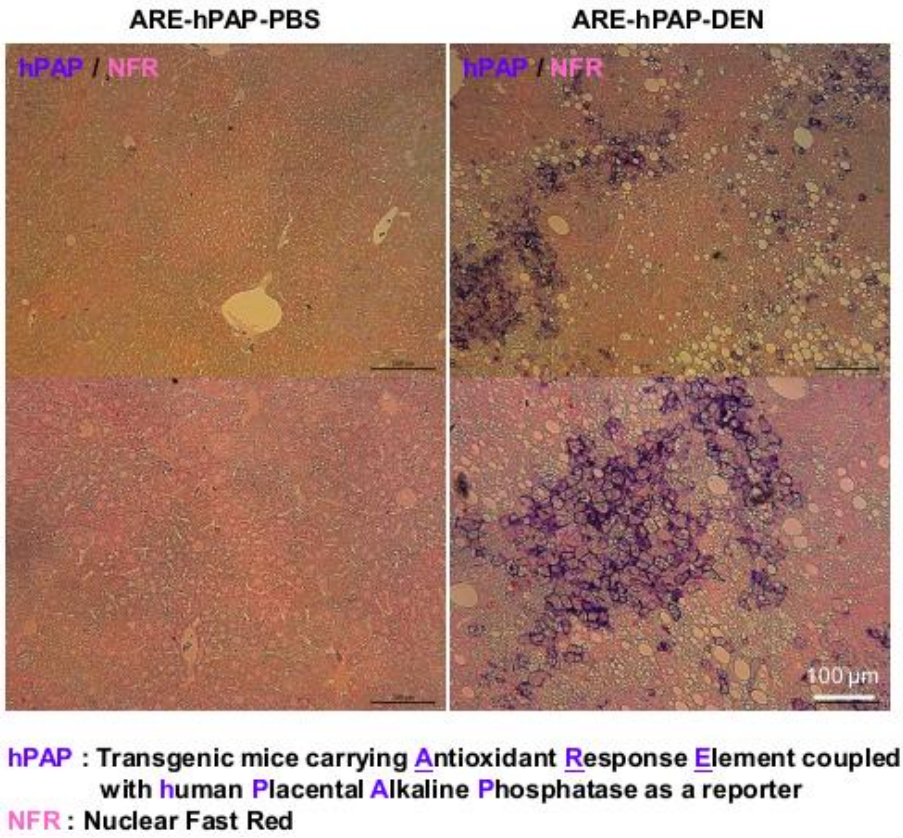

Figure 16. Nrf2 is overactivated in the hepatomas of DEN-treated WT mice. Paraffin-embedded liver sections from vehicle (PBS)- or DEN-treated ARE-hPAP mice at the age of 10 months were subjected to hPAP staining as described in Materials and Methods. Scale bars, 100 μm.

Nrf2 is required for hepatoma proliferation in the DEN-treated mice

Cell proliferation is a fundamental process required for cancer progression (66). Examination of liver sections of mice at 9 months after DEN injection revealed that proliferating cells stained with PCNA were heavily detected in the hepatomas from WT mice but rarely in adjacent normal tissues of WT mice or the livers of *Nrf2* KO mice (**Fig. 17**).

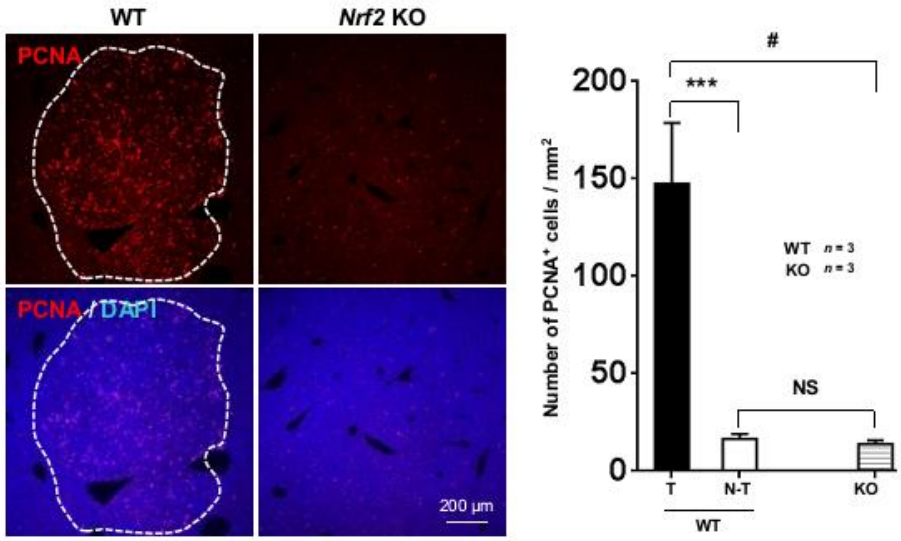

Figure 17. Nrf2 promotes cell proliferation in DEN-treated livers. Liver sections of WT and *Nrf2* KO mice treated with DEN at the age of 9 months were immunostained with PCNA antibody (left). The number of $PCNA^+$ cells per mm^2 in the indicated areas were counted and shown (n = 3 mice per genotype; right). DAPI was used to label cellular nuclei. Scale bars, 200 μm. Error bars show the SEM. $^{***}P < 0.001$, $^{\#}P < 0.0001$, NS: non-significant; two-tailed Student t test. Abbreviation: T, tumor; N-T, non tumor. DAPI was used to label cellular nuclei.

Similarly, Western blot analysis showed an increase in the protein level of cyclin D1 (**Fig. 18**) in WT livers but not in the livers of DEN-treated *Nrf2* KO mice. These observations suggested that Nrf2 is likely to drive DEN-induced hepatocarcinogenesis by stimulating hepatocyte proliferation.

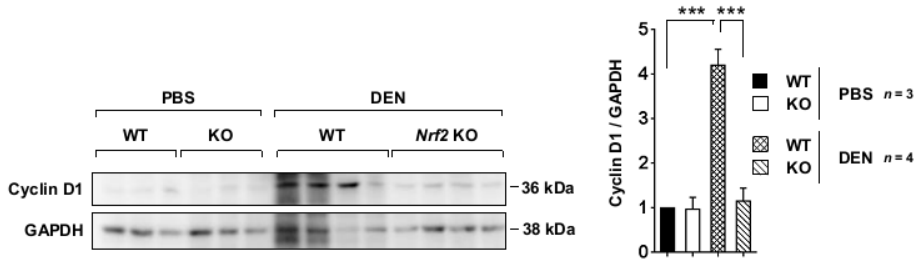

Figure 18. DEN injection results in overexpression of Cyclin D1 in livers of WT but not Nrf2 KO mice. Western blot analysis of livers from WT and *Nrf2* KO mice treated with vehicle [PBS; *n* (tissue) = 3 from 3 mice per genotype] or DEN [*n* (tissue) = 4 from 4 mice per genotype] at the age of 9 months showing an elevated level of cyclin D1 in the livers of DEN-treated WT mice but not *Nrf2* KO littermates. GAPDH was used as a loading control. The histogram represents quantification of cyclinD1 protein level. Error bars show the SEM. $^{***}P < 0.001$; two-tailed Student *t* test.

In an attempt to corroborate this speculation, I examined the short-term responses elicited by the DEN administration to WT and *Nrf2* KO mice. It has been well established that hepatocytes are quiescent in the normal liver, but acquire a remarkable capacity to proliferate in response to liver damage triggered by carcinogens or inflammatory insults. Not only does this mode of proliferation of surviving hepatocytes compensate for cell death to allow the maintenance of liver mass but also transmit genetic alterations to daughter cells in the favor of liver neoplastic progression, followed by dysplasia and later HCC development (67). Consistently, it has been firmly believed that compensatory hepatocyte proliferation is required for DEN-induced carcinogenesis (55,68). I therefore assessed hepatic proliferation in WT and *Nrf2* KO mice at the age of 15 days following DEN treatment for 48 hours. BrdU pulse-chase experiment and PCNA staining demonstrated the dramatically reduced compensatory proliferative response in the livers of *Nrf2* KO mice compared to WT mice (**Fig. 19**).

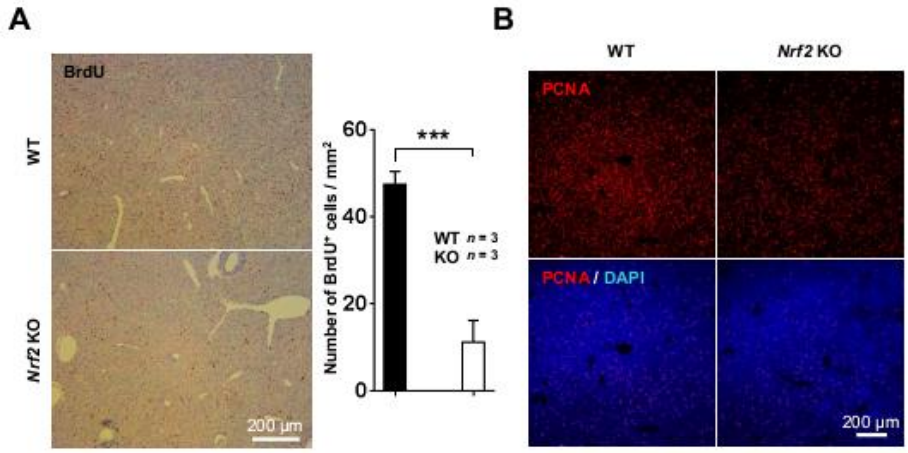

Figure 19. Nrf2 deficiency results in impaired compensatory proliferation. Liver sections of WT and *Nrf2* KO treated with DEN for 48 hours at the age of 15 days were subjected to BrdU (**C**; n = 3 mice per genotype) or PCNA staining (**D**, n =3 mice per genotype). The number of $BrdU^+$ cells per mm^2 were counted and shown. Scale bars, 200 μm. Error bars show the SEM. $^{***}P < 0.001$; two-tailed Student's t test. DAPI was used to label cellular nuclei.

In addition, I also examined the role of Nrf2 in hepatoma cell proliferation. In a colonogenic assay, the silencing of *Nrf2* by use of a specific small interfering RNA (siRNA) gave rise to decreased colony formation of hepatocellular carcinoma HepG2 (**Fig. 20A** and **B**) and Hep3B (**Fig. 20C** and **D**) cells. Collectively, the current study suggests that Nrf2 is necessary for cancer progression, presumably through stimulation of compensatory proliferation which subsequently enables hepatoma formation following DEN injection in mice.

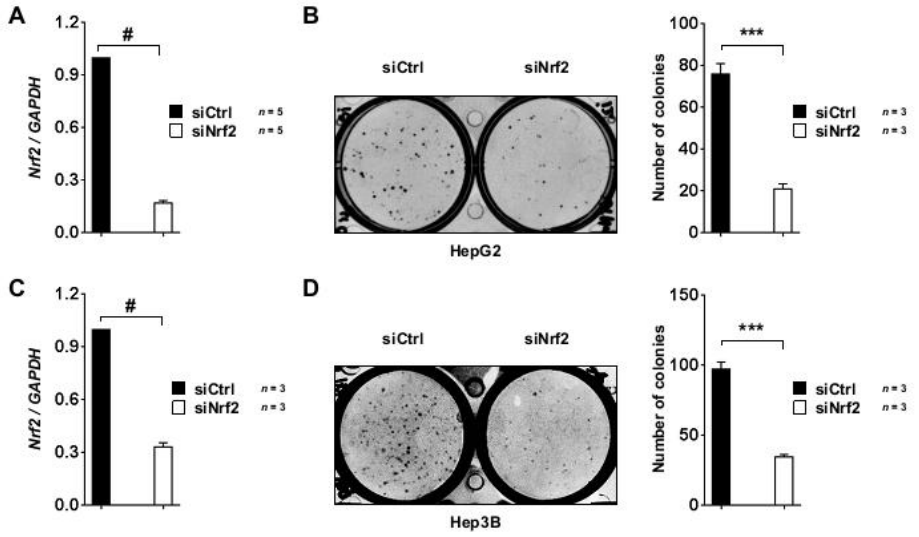

Figure 20. Silencing of *Nrf2* reduces colony formation in the hepatocellular carcinoma cells. HepG2 (**A**, **B**) and Hep3B (**C**, **D**) cells were transfected with either a control or a specific *Nrf2* siRNA. (**A**, **C**) Total RNA was extracted and analyzed by RT-PCR with *Nrf2* sequence-specific primers, verifying the silencing of *Nrf2*. GAPDH served as an internal control. (**B**, **D**) Transfected cells were subsequently subjected to colonogenic assays. Representative images were showed on the left and histograms (right) display the number of colonies counted (n = 3). Error bars show the SEM. $^{***}P < 0.001$, $^{\#}P < 0.0001$; two-tailed Student's t test.

Nrf2 enhances the expression of metabolic enzymes required for cell proliferation in hepatomas of DEN-treated mice

For the growth and proliferation of cancer cells, not only energy but also the building blocks including nucleotides are required, and they are synthesized only from glucose-derived precursors made in pentose phosphate pathway (PPP; ref.(69). Thus, it is not surprising to note that PPP plays an indispensable role in cancer progression and that PPP-related enzymes are frequently overexpressed in HCC (70,71). In line with this notion, suppressing these enzymes reportedly hampered HCC development (69-71). Notably, the expression of some key PPP-related enzymes is known to be Nrf2-dependent (72). Thus, I assessed the expression levels of the transporter of glucose uptake and representative PPP enzymes in the livers of WT and *Nrf2* KO mice that have been treated with DEN. I first noticed that the level of glucose transporter type 1 (*Glut1*) gene was markedly elevated in the livers of WT mice but not in those of in *Nrf2* KO littermates given DEN (**Fig. 21**).

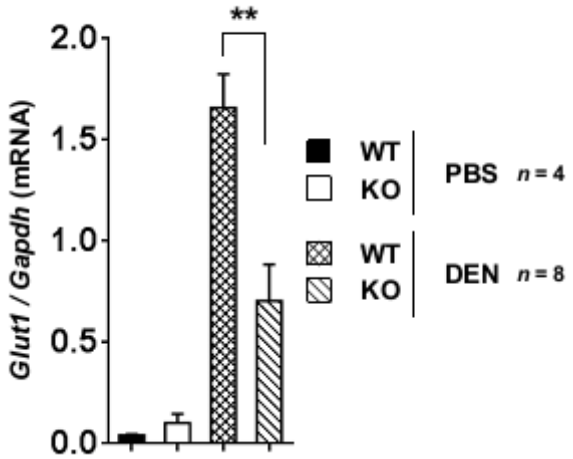

Figure 21. Glut1 is upregulated by Nrf2 in the livers of DEN-treated mice. RT-qPCR with specific primers were conducted to examine the mRNA level of *Glut1* in livers of either PBS- (the number of tissue samples = 4 from 4 mice per genotype) or DEN-treated (the number of tissue samples = 8 from 4 mice per genotype) WT and *Nrf2* KO mice at the age of 9 months. *Gapdh* served as an internal control. Data represent mean ± SEM. $^{**}P < 0.01$; two-tailed Student's *t* test.

The qPCR assay revealed that the hepatic expression levels of PPP metabolic genes encoding glucose-6-phosphate dehydrogenase (*G6pd*), phosphogluconate dehydrogenase (*Pgd*), transaldolase (*Taldo*) 1, transketolase (*Tkt*), malic enzyme (*Me*) 1, isocitrate dehydrogenase (*Idh1*) 1, phosphoribosyl pyrophosphate amidotransferase (*Ppat*), and methylenetetrahydrofolate dehydrogenase (*Mthfd*) 2 were markedly reduced in the DEN-treated *Nrf2* KO mice compared with those in WT animals subjected to the same treatment (**Fig. 22A**). Western blot analysis also confirmed that there was a profound downregulation of Pgd and Me1 in the livers of *Nrf2* KO mice treated with DEN (**Fig. 22B**).

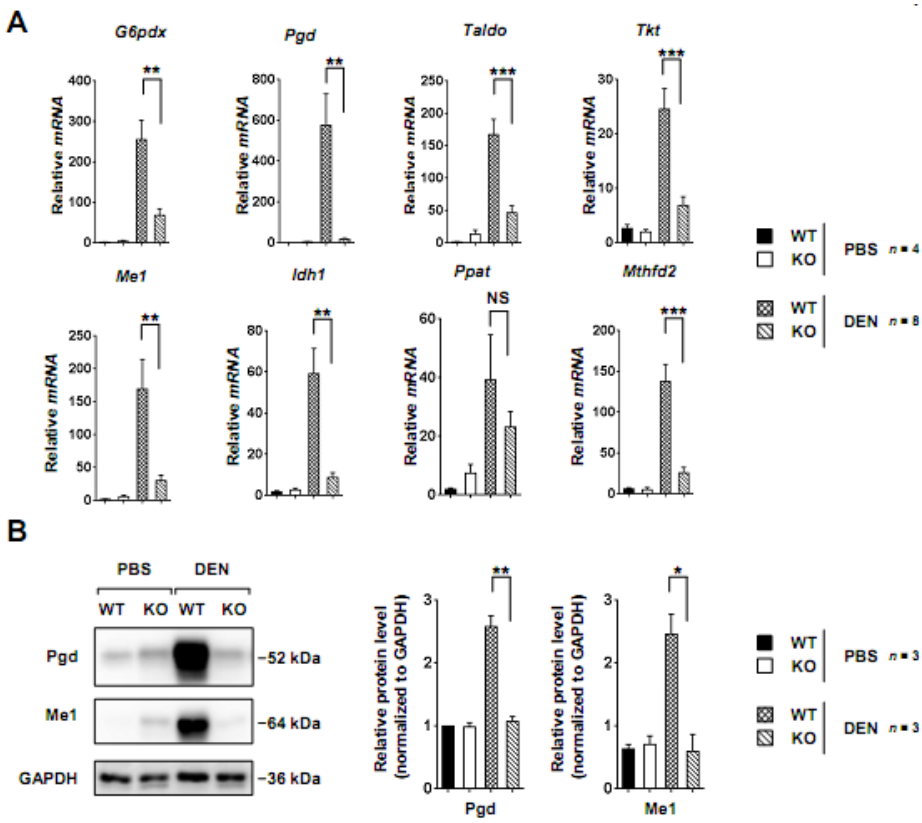

Figure 22. Nrf2 modulates the expression of PPP-related enzymes in the livers of DEN-treated mice. (A) RT-qPCR with specific primers were conducted to examine mRNA levels of indicated metabolic enzymes in the livers of vehicle [PBS; *n* (tissue) = 4 from 4 mice per genotype] or DEN-treated [*n* (tissue) = 8 from 4 mice per genotype] WT and *Nrf2* KO mice at the age of 9 months. mRNA levels of the indicated genes were normalized to that of *Gapdh* which served as an internal control. (**B**) Immunoblot analysis using liver tissue lysates from

9-month-old WT and *Nrf2* KO mice given PBS [*n* (tissue) = 3 from 3 mice per genotype] or DEN [*n* (tissue) = 3 from 3 mice per genotype]. GAPDH was used as a loading control. Data represent mean ± SEM. $^{*}P < 0.05$, $^{**}P < 0.01$, $^{***}P < 0.001$, $^{\#}P < 0.0001$, NS: non-significant; two-tailed Student's *t* test.

Nrf2 undergoes "gain-of-function" mutations during DEN-induced hepatocarcinogenesis

Mutations in the Keap1 binding domain of Nrf2 might prevent its degradation which arises from Keap1-binding in the cytoplasm. This will result in enhanced nuclear translocation of Nrf2 and subsequently its transcriptional activity by binding to ARE (42). Sequencing analysis of *Nrf2* in human HCC and experimentally induced rat HCC has revealed that *Nrf2* is commonly mutated in the region encoding the domain interacting with Keap1 (50,52). In agreement with this notion, I also noticed that *Nrf2* was mutated in DEN-induced HCC in mice, particularly in pairs of codons encoding amino acid residues 29 (80%) and 32 (100%) of its DLG motif (**Fig. 23A**). The Nrf2 levels in cells transfected with constructs expressing either murine or human *Nrf2*, which had been engineered to carry a single mutation in the codon encoding the amino acid residue 29, 32, or 80, were higher compared with those in cells harboring WT *Nrf2* (**Fig. 23B** and **C**). These findings suggest that mutations in the DLG motif of Nrf2 may account for its overactivation in the DEN-induced HCC.

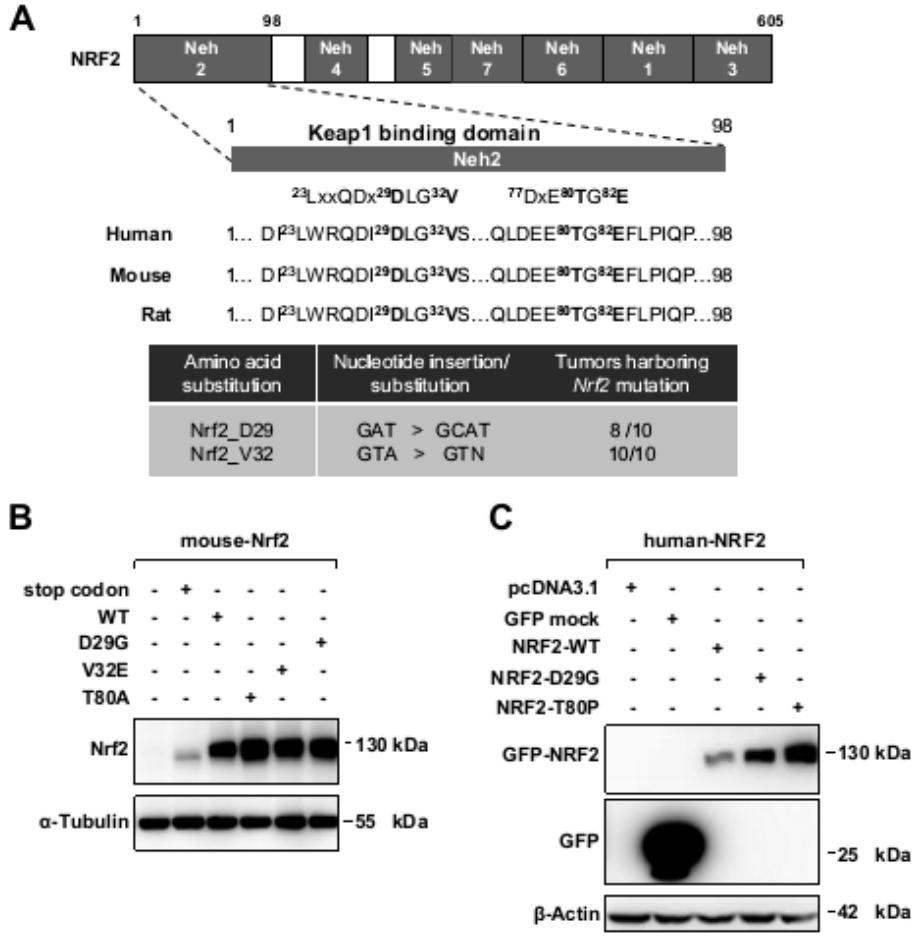

Figure 23. Mutations of *Nrf2* upregulate its protein expression. (A) cDNA prepared from livers of vehicle- and DEN-treated mice aged 9 months was subjected to sequencing analysis. Both nucleotide and amino acid substitutions are denoted. N: any nucleotide. (**B)** Various constructs expressing murine Nrf2 carrying indicated single point mutations were generated and transfected into HEK293T cells. Total

cell lysates were prepared and subjected to Western blot analysis with an antibody against Nrf2. Note an increase in the Nrf2 level due to these mutations. (**C**) Western blot analysis shows NRF2 levels in HEK293T cells exogenously expressing the indicated mutant forms of human NRF2. Data are the representative of three independent experiments.

I further assembled data from two independent studies of human HCC by AMC (56) and TCGA Research Network which have been deposited to the cBioPortal for Cancer Genomics (44,45) and analyzed for patients' survival rate. It is noticeable that median survival of HCC patients with WT *Nrf2* is longer than that of HCC counterparts carrying *Nrf2* mutations (**Fig. 24** and **Dataset 1**). Together, the data demonstrate that the Nrf2 activity in the hepatomas of mice given DEN was enhanced likely due to mutations including those in the Keap1 binding domain of *Nrf2* and the mutations in Nrf2 appeared to be associated with an inferior overal surivival.

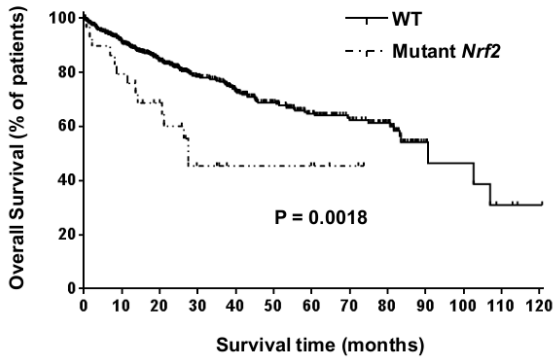

Figure 24. **Mutations in *Nrf2* are associated with an inferior survival**. Kaplan-Meier curves show overall survival of HCC patients with (n = 29) or without *Nrf2* mutations (n = 556). P = 0.0017, log-rank test

DISCUSSION

Nrf2 is a *bona fide* driver of liver cancer

Nrf2, the master regulator of cellular redox status is now being put at the heart of debate over its dual roles as a tumor suppressor and an oncogenic factor (73). Previous studies have demonstrated that deficiency of *Nrf2* renders animals more vulnerable to various types of carcinogens (58,74), while activating Nrf2 may reduce tumor burden (75). However, utilization of *Nrf2* KO mice allowed me to demonstrate the unexpected tumorigenic potential of Nrf2 in the DEN-induced murine HCC model. The current findings are in agreement with the recently reported observations that activation of Nrf2 promotes the progression lung (76), skin (77), and pancreatic cancers (31,78).

Many different typeas of cancers are known to express elaborated levels of ROS (79). It is crucial for cancer cells to maintain redox homeostasis as the excessive oxidative stress can also be detrimental to their survival (79). This strategy could be achieved by programmed expression of antioxidant enzymes that are mainly under the control of Nrf2. In line with this speculation, the progression of pancreatic cancer was promoted by K-Ras, B-Raf, and Myc oncogenes via the Nrf2-triggered antioxidant programs (78). The present study

also demonstrates that the expression levels of antioxidant genes including *Nqo1*, heme oxygenase 1 (*Hmox1*), and glutamate-cysteine ligase catalytic subunit (*Gclc*), whose transcription expression is under the tight control of Nrf2 (12), were elevated in the livers of WT mice but not *Nrf2* KO counterparts treated with DEN (**Fig. 25**).

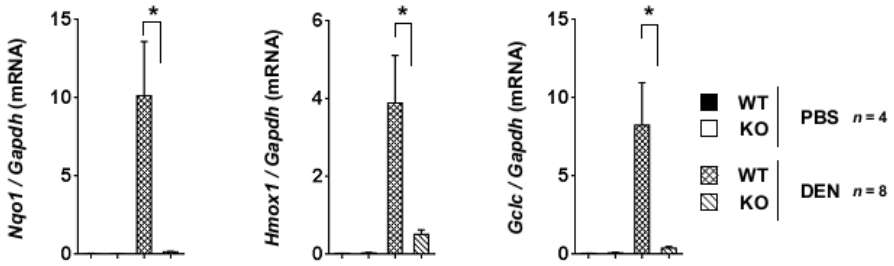

Figure 25. Nrf2 induces upregulation of hepatic antioxidant gene expression in the DEN-treated mice. RT-qPCR with specific primers were conducted to examine mRNA levels of indicated Nrf2 target genes in the livers of either PBS- (the number of tissue samples = 4 from 4 mice per genotype) or DEN-treated (the number of tissue samples = 8 from 4 mice per genotype) WT and *Nrf2* KO mice at the age of 9 months. *Gapdh* served as an internal control. Data represent mean ± SEM. $^{*}P < 0.05$, $^{***}P < 0.001$, $^{\#}P < 0.0001$; two-tailed Student's *t* test.

Redox status of cancer cells can also be modulated by the reduced form of nicotinamide adenine dinucleotide phosphate (NADPH), a reducing equivalent generated in the PPP (69). I noticed markedly elevated transcription levels of ARE-regulated PPP enzymes in the DEN-treated WT livers, but they were strongly suppressed in the livers of *Nrf2* KO mice given DEN. In addition to generating NADPH, the principal function of PPP is to produce phosphopentoses and ribonucleotides required for cell growth and proliferation (69). Therefore, the disparity in the extent of these metabolic enzymes in the livers of WT and *Nrf2* KO mice which have been treated with DEN might account for the difference in the tumor burden between these two genotypes. In agreement with the current observations, *Nrf2* Tg mice developed more tumors than their control littermates in a chemically induced skin carcinogenesis model due to the overexpression of ARE-mediated metabolic enzymes that favored the tumor cell growth (77). These findings suggest that the oncogenic function of Nrf2 is achieved, at least in part, through metabolic reprogramming towards anabolic glucose metabolism via the PPP.

It is noteworthy to mention that in another study, *Nrf2* mutant mice rather had sporadic congenital intrahepatic shunt, which evoked

an altered expression of Cyp2e1 and consequently reduced hepatotoxicity of acetaminophen whose bioactivation is also Cyp2e1-dependent (80). These finding may not be compatible with the current study. Although it is challenging to compare these two studies, I anticipate that the discrepancy might presumably be due, at least in part, to variations in strategies utilized to generate *Nrf2* mutant mice. *Nrf2* gene in the above study was disrupted using a positive-negative selection targeting vector whose *lacZ* cassette substitutes for part of exon 5 of *Nrf2*. This results in the deletion of 280 amino acids in carboxyl terminus of Nrf2, generating mutant Nrf2 with remaining N-terminal 301 residues linked to LacZ (8,80). In contrast, I used mice with part of exon 4 and all of exon 5 of *Nrf2* replaced with a reporter gene *lacZ* in the targeting vector. The replacement depletes the carboxyl 457 amino acids of Nrf2 and effectively nullifies the functions of *Nrf2* gene (53).

Nevertheless, remain there still questions that need addressing. In this study, the role of Nrf2 as a driver of hepatocarcinogenesis was investigated in a mouse model of HCC induced by DEN. Other murine HCC models with use of either other hepatocarcinogens such as aflatoxin (81) or genetically engineered mice (81) would be needed to

further testify these findings. In addition, the observation about the oncogenic potential of Nrf2 was made based on a long-term experiment, it would be necessary to dissect out the contribution of Nrf2 to HCC in the course of hepatocarcinogenesis, and possibly even in the context of involvement of other factors. It is also important to look at the interaction of Nrf2 with other proteins and factors in liver cancer, which is made much easier in the advent of availability of bioinformatics and big data.

In summary, the current findings reveal that Nrf2 serves as a key driver in DEN-induced hepatocarcinogenesis. In this disorder, Nrf2 gains its functions to enhance the expression of genes involved in the uptake and redistribution of glucose into PPP in order to support cancer cell growth as illustrated in Figure 26.

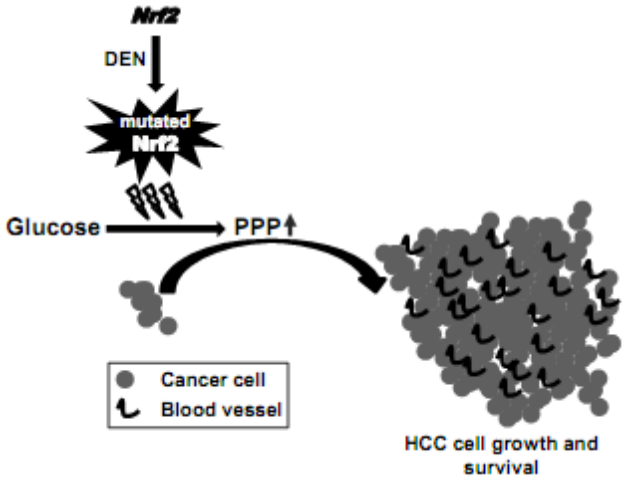

Figure 26. A proposed model for the role of Nrf2 in DEN-induced HCC. In DEN-induced murine HCC, Nrf2 is mutated to be overactivated. In response to Nrf2 overactivation, genes involving utilization and redistribution of glucose into PPP are upregulated to support rapid cancer cell proliferation. Abbreviation: DEN, diethylnitrosamine; HCC, hepatocellular carcinoma; PPP, pentose phosphate pathway.

Nrf2 is also an oncoprotein in other cancers

The fact that Nrf2/ARE activates the expression of phase II and antioxidant enzymes to eliminate excessive electrophiles and ROS and favor the survival of normal cells would be logically extended to cancer cells (73). Mild oxidative stress plays a role as an important intracellular signaling molecule to promote cell proliferation and is involved in the maintenance of the oncogenic phenotypes (82), whereas ROS accumulated in excess would be a strategy to target cancer cells (83). Hence activating Nrf2 is an elegant tactic evolved by cancer cells to survive imbalanced redox homeostasis arising from aberrantly high metabolism rate (82). It has been reported that endogenous expression of oncogenic alleles of *Kras* (K-Ras^{G12D}), *Braf* (B-Raf^{V619E}) and *Myc* (Myc^{ERT2}) transcriptionally induces the expression of Nrf2, which then results in a favorable intracellular environment for tumor cell survival with a lower level of ROS (78). As a consequence, genetic deletion of *Nrf2* greatly impaired K-Ras^{G12D}-induced murine lung and pancreatic cancers (78). The protective effects of Nrf2 against oxidative stress are applied to proteins, in which Nrf2 allows the cysteine residues in protein components of the mRNA translation machinery to maintain the reduced status, securing pancreatic cancer cell proliferation and

maintenance (31). A groundbreaking research by Mitsuishi et al. revealed that Nrf2 could be hijacked by cancer cells to redistribute glucose and glutamine towards the anabolic pathway to meet energy demand for rapid growth of cancer cells (72). Mutations in *Nrf2* including amplification and substitutions clustered in a gene region coding for amino acids in DLG and ETGE motifs are closely related to a poor clinical outcome. Squamous cell lung carcinoma patients with these activating genetic alterations in *Nrf2* showed a shorter disease-free survival compared to their cohort with wild-type *Nrf2* (42). The similar segregation was observed in esophageal squamous cancer (84). This suggests the oncogenic potential of "gain-of-function" or activated Nrf2 and puts chronically sustained activation of Nrf2 on high alert and urgently calls for an approachable intervention in case of cancer with overactivated Nrf2.

Future direction: Nrf2 as a target of precision oncology for cancer prognosis and treatment

As Nrf2 appears to serve as an oncogenic factor in cancer, deletion of *Nrf2* might alleviate cancer progression. However, Nrf2 is required for maintenance of physiological redox homeostasis, hence harnessing but

not completely deleting *Nrf2* might be a better strategy for cancer therapy. Moreover, Nrf2 overactivation often occurs as a consequence of its mutations by environmental carcinogens rather than amplification of its normal gene, so it might be a more fundamental preventive strategy to avoid genetoxic insults damaging Nrf2 and/or its regulator Keap1. An increasing body of evidence has suggested that the oncogenic potential of Nrf2 lies in its "gain-of-function" mutations, which heavily cluster in region encoding Keap1 binding motifs DLG and ETGE motifs. Therefore, correcting these mutations may delay the Nrf2-dependent cancer cell growth and tumor progression. In this context, it is interesting to note that replenishment of tumor suppressor gene adenomatous polyposis coli (*APC*), which is frequently mutated and inactivated in colorectal cancer, help promote differentiation of colon cancer cells and reverse colon cancer in mice (85).

It is also noticeable that mutations in *Nrf2* are related to shorter survival time in many types of cancer. Therefore, *Nrf2* mutation testing and/or profiling *Nrf2* should be recommended as part of every single clinical practice guideline to categorize patients into groups with or without genetic alterations in *Nrf2* and subsequently determine precision therapy for associated cancer patients (**Fig. 27**).

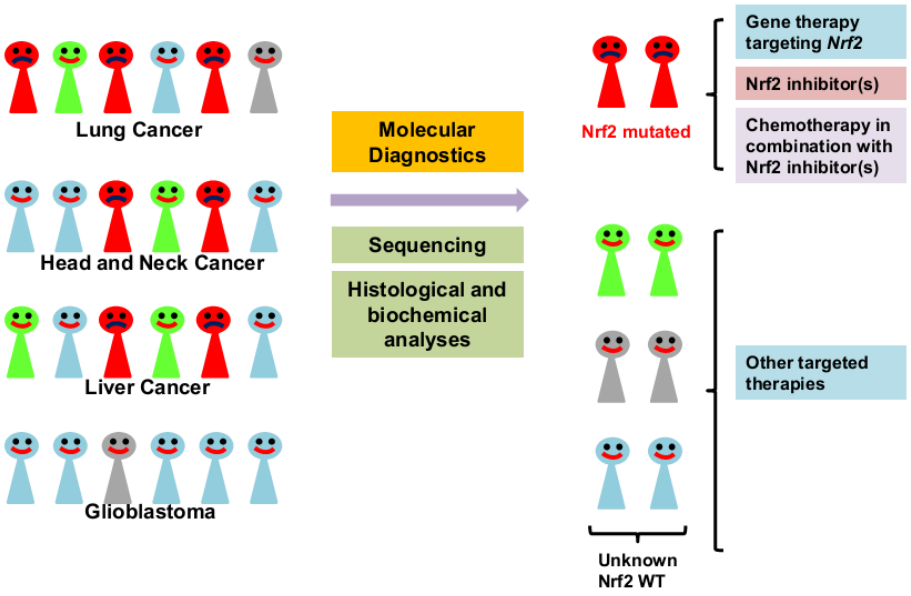

Figure 27. The introduction of Nrf2 in precision cancer therapy. Tumor tissues form various types of cancer can be subjected to a series of molecular diagnostics including histological and biological analyses to evaluate Nrf2 levels as well as the magnitude/frequency of genetic alterations. Individuals with genetically altered *Nrf2* then would be distinguished and grouped to guide the selection of more appropriate drugs for such the group.

Strategies to identify genetic alterations of **Nrf2** *in cancer*

It is now conceivable that tumors are heterogeneous. Within a tumor, cancer cells might not be all the same (intratumor heterogeneity) and tumors of a given cancer type could be drastically different from patient to patient (intertumor heterogeneity) in terms of genetic alterations (86-88). Intratumor heterogeneity might arise from clonal evolution through which selection upon exposure to given therapies gives rise to a pool of mutations. Intratumor heterogeneity hence could explain the relapse as well as the development of polyclonal resistance in the course of treatment in some patients who initially have a good response to a given cancer drug. Whilst, the variations among individuals with the same type of cancer determine which subgroup would benefit from a targeted therapy (86,88). Understanding distinct features of every single tumor cell would provide a basis for personalized anticancer therapy in the new era of precision medicine (89-91). Current advances in characterizing patients and their tumors by use of genomics, proteomics, and metabolomics and the availability of large-scale clinical genomic database as well as supercomputers used to interpret big data have enabled classification of patients and determination of a more precise treatment with maximal efficacy and minimal toxicity (89,92). The

success of precision cancer medicine rests heavily on the identification of validated molecular variations specific to each patient known as biomarkers (93).

The regularity of genetic alterations in *Nrf2* in cancer as well as their association with an inferior clinical outcome might suggest that this transcriptional factor would serve as a biomarker in precision cancer medicine. In this context, profiling *Nrf2* would be recommended being included in cancer management, encompassing initial diagnosis, risk stratification, disease prognosis, predicting responses to treatment, and finally deciding more precise medication for corresponding individuals. A drop in the cost and advances in high-throughput next-generation sequencing technology have made characterization of genetic aberrations in *Nrf2* easier than ever (94,95). Nevertheless, the pitfall remains to be addressed here is that *Nrf2* profiling has been so far conducted on the entire needle biopsies collected through tumor removal (42,51), which might not represent the whole tumor genomic landscape due to intratumor heterogeneity (88). Single-cell DNA and RNA sequencing (SCS) methods developed and revolutionized lately (96-98) would be applied to obtain a new powerful approach for narrowing understanding any alterations in *Nrf2* in every tumor cell

rather than in the entire tumor mass (96,97). SCS for characterizing *Nrf2* would be also extended to circulating tumor cells (CTC), which are sloughed from primary tumors and carry even additional acquired mutations as a result of exposure to therapeutic treatment in a metastatic context (99,100). In addition to CTC, tumor-derived circulating-tumor DNA (ctDNA) present in blood or other body fluids (101), which has been noticed to well correlate with changes in tumor load (102-104), should be encouraged to be subjected to *Nrf2* profiling. CTC and ctDNA are attractive noninvasive alternatives to tumor biopsies, and may reflect real-time tumor burden during the course of cancer treatment (105-107).

Chemotherapy to modulate Keap1/Nrf2/ARE axis in Nrf2 mutant-bearing cancer cells

A major hurdle toward precision cancer medicine is the development of therapeutic agents that are paired with validated biomarkers (90,92). The characterization of *Nrf2* mutation as a new biomarker in a plethora of cancer types might pave the way for further classification of cancer into subtypes negative or positive for *Nrf2* aberrations, which are distinctive in clinical outcomes and apparently response to treatment. In

such cases of subclasses addicted to Nrf2, molecules targeting Nrf2 would be considered of particular interest. Reagents including phytochemicals that activate Nrf2 have been long developed in an attempt to active Nrf2 in normal cells for chemoprevention (12). On the other hand, the increasingly recognized oncogenic roles of constitutively activated Nrf2 in transformed or cancerous cells have shifted researchers' attention to the path toward developing Nrf2 inhibitors. However, unlike thousands of verified Nrf2 activators, only a small number of Nrf2 inhibitors have been identified so far (108,109), but none of them is available for clinical use currently. A lack in fully resolved crystal structure of Nrf2 might be the reason why developing Nrf2 inhibitors is in its infancy.

Gene-based therapies to target mutant Nrf2 in cancer cells

Strategies to attenuate activated Nrf2

It is noteworthy that sustained activation of Nrf2 lies in its genetic alterations, which encompass DNA amplification and somatic point mutations, suggesting gene therapy targeting *Nrf2*. Gene-based therapies are basically the introduction of exogenous nucleic acids to cancer cells in order to restore the functions of genes that are missing or

to halt the expression of tumor-promoting genes (110). RNA interference (RNAi) which selectively inhibits translation of mRNA transcript of a target gene into a protein has been being broadly harnessed for clinical applications and particularly in cases considered ‘undruggable’ (111,112), could be hold promises for cancer with *Nrf2* amplified. Despite encouraging outcomes from recent clinical trials, RNAi therapeutics have some limitations. These include: a need for safe and efficient methods to deliver RNAi to the site-of-action without posing adverse effects on non-target cells, possible off-target- and immunostimulatory effects (113). Thus, RNAi specific to *Nrf2* should be developed with meticulous attention.

Correction of substitution mutations by programmable nuclease-based genome editing technologies

As a fascinating addition to RNAi therapy, the introduction of programmable nucleases-based genome editing technologies have paved the way for easier and more efficient deletion or correction of genetic aberrations. The principle to achieve genome precisely edited is to introduce DNA-double stranded breaks (DSBs) by nucleases at genomic locus of interest. Thereafter, either nonhomologous end-

joining (NHEJ) or homology-directed repair (HDR) in the presence of single-stranded oligonucleotides (ssODNs) homologous to the targeted region is activated to seal the breaks. NHEJ results in insertion/deletion mutations (indel) (114,115), which disrupts the target genes. DSBs followed by NHEJ, in consequence, could be introduced to eradicate amplified *Nrf2* in cancer. HDR allows the exchange of nucleotide sequence between targeted DNA strands and ssODN donor templates, leading to the introduction of point mutations desired or insertion of sequences of choice (114,116). DSBs with ssODNs on the one hand allow the insertion of additional mutations to bZIP-Maf in *Nrf2*, which interferes with the interaction of Nrf2 and ARE to attenuate the enhanced transcriptional activity of functionally activated Nrf2 in cancer. On the other hand, this mechanism also would facilitate the correction of activating substitutions in DLG and ETGE motifs of Nrf2, turning Keap1-resistant activated Nrf2 to the wild-type one that is tightly regulated by Keap1. Currently, four classes of nucleases, including three protein-based systems, which are meganucleases, zinc finger nucleases (ZFNs) and transcription activator-like effector nucleases (TALENs), are available. Because the recognition of specific genomic sites by the first three nucleases is based on protein-DNA

interactions, different specific nucleases need to be complicatedly engineered for different target sequences. The clustered regularly interspaced short palindromic repreats (CRISPR)-associated protein (Cas) 9 system which has been invented recently is much more flexible and ready-to-use as it works on the basis of interaction between an engineered short RNA guide and the target DNA site (114,116). Hence, the RNA-based CRISPR-cas9 system would be strongly urged to be considered as a powerful tool to achieve the desired changes in *Nrf2* including elimination and correction of point mutations.

A need for drug combinations and drug evaluation to precisely target Nrf2 for cancer treatment

A tumor bulk is heterogeneous with a myriad of mutations arising in the course of tumor evolution (86,117). Concordantly, in various types of cancer, genetic alterations in *Nrf2* are temporally accompanied by changes of other genes, which might occur at different stages of tumor development (118-120). It is apparent to tolerate that behaviors of mutated *Nrf2* in cancer would be dictated by genetic landscape as well as co-coexisting mutations, which is termed epistatic interactions (117). Understanding genetic background would thereby provide an elegant

platform for optimizing the combination of not only ‘drugs’ targeting activated *Nrf2* and but also those for other concomitant aberrations to achieve the desired therapeutic effects (87).

Although Nrf2 could serve as an attractive therapeutic target for cancer treatment, the Nrf2-based aforementioned therapies would not be given precisely to the right patients unless the vulnerabilities of live patient cancer cells to potential drugs are verified (91). To date, there have been many methods developed to obtain the sufficient number of patient-derived live cancer cells for ‘drug’ testing. These include conditional reprogramming, which involves in the using an enriched environment to expand the human tissues, cultivating patient cancer cells in a semi-solid extracellular matrix three-dimentional (3D) condition to allow formation of organoids (121,122), and enrichment of CTCs on an advanced microfluidic chip (123). Various functional analyses have been also invented for measuring drug effects on patients’ live cancer cells such as utilizing patient-derived xenograft (PDX) mouse models (91). This functional testing would be included to facilitate the development of therapies targeting Nrf2 and the guidance on precisely matched therapies.

Conclusions

Despite the fact that whether Nrf2 is a tumor suppressor or an oncogene has been an unsolved conundrum, it is becoming apparent that Nrf2 actively secures maintenance of fully malignant cells and therefore exacerbating cancer progression cancer progression(31,73). Constitutive overactivation of Nrf2 is speculated to regulate metabolic reprogramming to meet the anabolic needs for rapid cell proliferation(30,72), and to create a favorable microenvironment with less oxidative stress for cancer cell growth via the overexpression of phase II-detoxifying and antioxidant enzymes(78). These tumorigenic potentials of Nrf2 lie in its sustained activation in cancer, which is speculated to arise from two 'hot-spots' gain-of-function mutations located in the DLG and ETGE motifs in the Neh2 domain(124). As these aberrations of *Nrf2* are so ubiquitous and involves in behavior and vulnerability to chemotherapies in a medley of cancer types, they could be supposed to be an attractive target for precision cancer therapy. However, it still remains questioned to what extent these genetic changes and hot-spot mutations of *Nrf2* contributes to cancer progression. For targeting Nrf2, it is critical to profile the genotype of this transcription factor in every single cell from either tumor bulks or

CTCs, and not to mention, to consider the not only *Nrf2* but the entire genetic background as they might define behaviors of Nrf2.

REFERENCES

1. Miller EC, Miller JA. Mechanisms of chemical carcinogenesis. Cancer **1981**;47(5 Suppl):1055-64.

2. Miller JA. Carcinogenesis by chemicals: an overview--G. H. A. Clowes memorial lecture. Cancer Res **1970**;30(3):559-76.

3. Benson AM, Batzinger RP, Ou SY, Bueding E, Cha YN, Talalay P. Elevation of hepatic glutathione S-transferase activities and protection against mutagenic metabolites of benzo(a)pyrene by dietary antioxidants. Cancer Res **1978**;38(12):4486-95.

4. Carroll RE, Benya RV, Turgeon DK, Vareed S, Neuman M, Rodriguez L, *et al.* Phase IIa clinical trial of curcumin for the prevention of colorectal neoplasia. Cancer Prev Res (Phila) **2011**;4(3):354-64.

5. Rushmore TH, Morton MR, Pickett CB. The antioxidant responsive element. Activation by oxidative stress and identification of the DNA consensus sequence required for functional activity. J Biol Chem **1991**;266(18):11632-9.

6. Xie T, Belinsky M, Xu Y, Jaiswal AK. ARE- and TRE-mediated regulation of gene expression. Response to xenobiotics and antioxidants. J Biol Chem **1995**;270(12):6894-900.

7. Moi P, Chan K, Asunis I, Cao A, Kan YW. Isolation of NF-E2-related factor 2 (Nrf2), a NF-E2-like basic leucine zipper transcriptional activator that binds to the tandem NF-E2/AP1 repeat of the beta-globin locus control region. Proc Natl Acad

Sci U S A **1994**;91(21):9926-30.

8. Itoh K, Chiba T, Takahashi S, Ishii T, Igarashi K, Katoh Y, *et al.* An Nrf2/small Maf heterodimer mediates the induction of phase II detoxifying enzyme genes through antioxidant response elements. Biochem Biophys Res Commun **1997**;236(2):313-22.

9. Xu Z, Wang S, Ji H, Zhang Z, Chen J, Tan Y, *et al.* Broccoli sprout extract prevents diabetic cardiomyopathy via Nrf2 activation in db/db T2DM mice. Sci Rep **2016**;6:30252.

10. Howden R. Nrf2 and cardiovascular defense. Oxid Med Cell Longev **2013**;2013:104308.

11. Xiong W, MacColl Garfinkel AE, Li Y, Benowitz LI, Cepko CL. NRF2 promotes neuronal survival in neurodegeneration and acute nerve damage. J Clin Invest **2015**;125(4):1433-45.

12. Surh YJ. Cancer chemoprevention with dietary phytochemicals. Nat Rev Cancer **2003**;3(10):768-80.

13. Jaramillo MC, Zhang DD. The emerging role of the Nrf2-Keap1 signaling pathway in cancer. Genes Dev **2013**;27(20):2179-91.

14. Itoh K, Wakabayashi N, Katoh Y, Ishii T, Igarashi K, Engel JD, *et al.* Keap1 represses nuclear activation of antioxidant responsive elements by Nrf2 through binding to the amino-terminal Neh2 domain. Genes Dev **1999**;13(1):76-86.

15. Tong KI, Katoh Y, Kusunoki H, Itoh K, Tanaka T, Yamamoto M. Keap1 recruits Neh2 through binding to ETGE and DLG motifs: characterization of the two-site molecular recognition

model. Mol Cell Biol **2006**;26(8):2887-900.

16. Nioi P, Nguyen T, Sherratt PJ, Pickett CB. The carboxy-terminal Neh3 domain of Nrf2 is required for transcriptional activation. Mol Cell Biol **2005**;25(24):10895-906.
17. Katoh Y, Itoh K, Yoshida E, Miyagishi M, Fukamizu A, Yamamoto M. Two domains of Nrf2 cooperatively bind CBP, a CREB binding protein, and synergistically activate transcription. Genes Cells **2001**;6(10):857-68.
18. Salazar M, Rojo AI, Velasco D, de Sagarra RM, Cuadrado A. Glycogen synthase kinase-3beta inhibits the xenobiotic and antioxidant cell response by direct phosphorylation and nuclear exclusion of the transcription factor Nrf2. J Biol Chem **2006**;281(21):14841-51.
19. McMahon M, Thomas N, Itoh K, Yamamoto M, Hayes JD. Redox-regulated turnover of Nrf2 is determined by at least two separate protein domains, the redox-sensitive Neh2 degron and the redox-insensitive Neh6 degron. J Biol Chem **2004**;279(30):31556-67.
20. Rada P, Rojo AI, Chowdhry S, McMahon M, Hayes JD, Cuadrado A. SCF/{beta}-TrCP promotes glycogen synthase kinase 3-dependent degradation of the Nrf2 transcription factor in a Keap1-independent manner. Mol Cell Biol **2011**;31(6):1121-33.
21. Wang H, Liu K, Geng M, Gao P, Wu X, Hai Y, *et al.* RXRalpha inhibits the NRF2-ARE signaling pathway through a direct interaction with the Neh7 domain of NRF2. Cancer Res

2013;73(10):3097-108.

22. Dinkova-Kostova AT, Holtzclaw WD, Cole RN, Itoh K, Wakabayashi N, Katoh Y, *et al.* Direct evidence that sulfhydryl groups of Keap1 are the sensors regulating induction of phase 2 enzymes that protect against carcinogens and oxidants. Proc Natl Acad Sci U S A **2002**;99(18):11908-13.
23. Wakabayashi N, Dinkova-Kostova AT, Holtzclaw WD, Kang MI, Kobayashi A, Yamamoto M, *et al.* Protection against electrophile and oxidant stress by induction of the phase 2 response: fate of cysteines of the Keap1 sensor modified by inducers. Proc Natl Acad Sci U S A **2004**;101(7):2040-5.
24. Zipper LM, Mulcahy RT. The Keap1 BTB/POZ dimerization function is required to sequester Nrf2 in cytoplasm. J Biol Chem **2002**;277(39):36544-52.
25. Cullinan SB, Gordan JD, Jin J, Harper JW, Diehl JA. The Keap1-BTB protein is an adaptor that bridges Nrf2 to a Cul3-based E3 ligase: oxidative stress sensing by a Cul3-Keap1 ligase. Mol Cell Biol **2004**;24(19):8477-86.
26. Furukawa M, Xiong Y. BTB protein Keap1 targets antioxidant transcription factor Nrf2 for ubiquitination by the Cullin 3-Roc1 ligase. Mol Cell Biol **2005**;25(1):162-71.
27. Sayin VI, Ibrahim MX, Larsson E, Nilsson JA, Lindahl P, Bergo MO. Antioxidants accelerate lung cancer progression in mice. Sci Transl Med **2014**;6(221):221ra15.
28. Le Gal K, Ibrahim MX, Wiel C, Sayin VI, Akula MK, Karlsson C, *et al.* Antioxidants can increase melanoma metastasis in mice. Sci Transl Med **2015**;7(308):308re8.

29. Wang H, Liu X, Long M, Huang Y, Zhang L, Zhang R, *et al.* NRF2 activation by antioxidant antidiabetic agents accelerates tumor metastasis. Sci Transl Med **2016**;8(334):334ra51.

30. DeNicola GM, Chen PH, Mullarky E, Sudderth JA, Hu Z, Wu D, *et al.* NRF2 regulates serine biosynthesis in non-small cell lung cancer. Nat Genet **2015**;47(12):1475-81.

31. Chio, II, Jafarnejad SM, Ponz-Sarvise M, Park Y, Rivera K, Palm W, *et al.* NRF2 Promotes Tumor Maintenance by Modulating mRNA Translation in Pancreatic Cancer. Cell **2016**;166(4):963-76 .

32. Yang C, Tan YX, Yang GZ, Zhang J, Pan YF, Liu C, *et al.* Gankyrin has an antioxidative role through the feedback regulation of Nrf2 in hepatocellular carcinoma. J Exp Med **2016**;213(5):859-75.

33. Jiang T, Chen N, Zhao F, Wang XJ, Kong B, Zheng W, *et al.* High levels of Nrf2 determine chemoresistance in type II endometrial cancer. Cancer Res **2010**;70(13):5486-96.

34. Konstantinopoulos PA, Spentzos D, Fountzilas E, Francoeur N, Sanisetty S, Grammatikos AP, *et al.* Keap1 mutations and Nrf2 pathway activation in epithelial ovarian cancer. Cancer Res **2011**;71(15):5081-9.

35. Hayes JD, McMahon M. NRF2 and KEAP1 mutations: permanent activation of an adaptive response in cancer. Trends Biochem Sci **2009**;34(4):176-88.

36. Ikeda H, Nishi S, Sakai M. Transcription factor Nrf2/MafK regulates rat placental glutathione S-transferase gene during hepatocarcinogenesis. Biochem J **2004**;380(Pt 2):515-21.

37. Stacy DR, Ely K, Massion PP, Yarbrough WG, Hallahan DE, Sekhar KR, *et al.* Increased expression of nuclear factor E2 p45-related factor 2 (NRF2) in head and neck squamous cell carcinomas. Head Neck **2006**;28(9):813-8.

38. Wang XJ, Sun Z, Villeneuve NF, Zhang S, Zhao F, Li Y, *et al.* Nrf2 enhances resistance of cancer cells to chemotherapeutic drugs, the dark side of Nrf2. Carcinogenesis **2008**;29(6):1235-43.

39. Padmanabhan B, Tong KI, Ohta T, Nakamura Y, Scharlock M, Ohtsuji M, *et al.* Structural basis for defects of Keap1 activity provoked by its point mutations in lung cancer. Mol Cell **2006**;21(5):689-700.

40. Singh A, Misra V, Thimmulappa RK, Lee H, Ames S, Hoque MO, *et al.* Dysfunctional KEAP1-NRF2 interaction in non-small-cell lung cancer. PLoS Med **2006**;3(10):e420.

41. Wang R, An J, Ji F, Jiao H, Sun H, Zhou D. Hypermethylation of the Keap1 gene in human lung cancer cell lines and lung cancer tissues. Biochem Biophys Res Commun **2008**;373(1):151-4.

42. Shibata T, Ohta T, Tong KI, Kokubu A, Odogawa R, Tsuta K, *et al.* Cancer related mutations in NRF2 impair its recognition by Keap1-Cul3 E3 ligase and promote malignancy. Proc Natl Acad Sci U S A **2008**;105(36):13568-73.

43. Kim YR, Oh JE, Kim MS, Kang MR, Park SW, Han JY, *et al.* Oncogenic NRF2 mutations in squamous cell carcinomas of oesophagus and skin. J Pathol **2010**;220(4):446-51.

44. Cerami E, Gao J, Dogrusoz U, Gross BE, Sumer SO, Aksoy BA, *et al.* The cBio cancer genomics portal: an open platform for exploring multidimensional cancer genomics data. Cancer Discov **2012**;2(5):401-4.
45. Gao J, Aksoy BA, Dogrusoz U, Dresdner G, Gross B, Sumer SO, *et al.* Integrative analysis of complex cancer genomics and clinical profiles using the cBioPortal. Sci Signal **2013**;6(269):pl1.
46. Fukutomi T, Takagi K, Mizushima T, Ohuchi N, Yamamoto M. Kinetic, thermodynamic, and structural characterizations of the association between Nrf2-DLGex degron and Keap1. Mol Cell Biol **2014**;34(5):832-46.
47. Chowdhry S, Zhang Y, McMahon M, Sutherland C, Cuadrado A, Hayes JD. Nrf2 is controlled by two distinct beta-TrCP recognition motifs in its Neh6 domain, one of which can be modulated by GSK-3 activity. Oncogene **2013**;32(32):3765-81.
48. Zucman-Rossi J, Villanueva A, Nault JC, Llovet JM. Genetic Landscape and Biomarkers of Hepatocellular Carcinoma. Gastroenterology **2015**;149(5):1226-39.
49. Laursen L. A preventable cancer. Nature **2014**;516(7529):S2-3.
50. Guichard C, Amaddeo G, Imbeaud S, Ladeiro Y, Pelletier L, Maad IB, *et al.* Integrated analysis of somatic mutations and focal copy-number changes identifies key genes and pathways in hepatocellular carcinoma. Nat Genet **2012**;44(6):694-8.
51. Fujimoto A, Furuta M, Totoki Y, Tsunoda T, Kato M, Shiraishi Y, *et al.* Whole-genome mutational landscape and characterization of noncoding and structural mutations in liver

cancer. Nat Genet **2016**;48(5):500-9.

52. Zavattari P, Perra A, Menegon S, Kowalik MA, Petrelli A, Angioni MM, *et al.* Nrf2, but not beta-catenin, mutation represents an early event in rat hepatocarcinogenesis. Hepatology **2015**;62(3):851-62.

53. Chan K, Lu R, Chang JC, Kan YW. NRF2, a member of the NFE2 family of transcription factors, is not essential for murine erythropoiesis, growth, and development. Proc Natl Acad Sci U S A **1996**;93(24):13943-8.

54. Johnson DA, Andrews GK, Xu W, Johnson JA. Activation of the antioxidant response element in primary cortical neuronal cultures derived from transgenic reporter mice. J Neurochem **2002**;81(6):1233-41.

55. Naugler WE, Sakurai T, Kim S, Maeda S, Kim K, Elsharkawy AM, *et al.* Gender disparity in liver cancer due to sex differences in MyD88-dependent IL-6 production. Science **2007**;317(5834):121-4.

56. Ahn SM, Jang SJ, Shim JH, Kim D, Hong SM, Sung CO, *et al.* Genomic portrait of resectable hepatocellular carcinomas: implications of RB1 and FGF19 aberrations for patient stratification. Hepatology **2014**;60(6):1972-82.

57. Hacker HJ, Mtiro H, Bannasch P, Vesselinovitch SD. Histochemical profile of mouse hepatocellular adenomas and carcinomas induced by a single dose of diethylnitrosamine. Cancer Res **1991**;51(7):1952-8.

58. Becks L, Prince M, Burson H, Christophe C, Broadway M, Itoh K, *et al.* Aggressive mammary carcinoma progression in Nrf2 knockout mice treated with 7,12-dimethylbenz[a]anthracene. BMC Cancer **2010**;10:540.

59. Verna L, Whysner J, Williams GM. N-nitrosodiethylamine mechanistic data and risk assessment: bioactivation, DNA-adduct formation, mutagenicity, and tumor initiation. Pharmacol Ther **1996**;71(1-2):57-81.

60. Kang JS, Wanibuchi H, Morimura K, Gonzalez FJ, Fukushima S. Role of CYP2E1 in diethylnitrosamine-induced hepatocarcinogenesis in vivo. Cancer Res **2007**;67(23):11141-6.

61. Oinonen T, Lindros KO. Zonation of hepatic cytochrome P-450 expression and regulation. Biochem J **1998**;329 (Pt 1):17-35.

62. Wiench K, Frei E, Schroth P, Wiessler M. 1-C-glucuronidation of N-nitrosodiethylamine and N-nitrosomethyl-n-pentylamine in vivo and in primary hepatocytes from rats pretreated with inducers. Carcinogenesis **1992**;13(5):867-72.

63. Buckley DB, Klaassen CD. Induction of mouse UDP-glucuronosyltransferase mRNA expression in liver and intestine by activators of aryl-hydrocarbon receptor, constitutive androstane receptor, pregnane X receptor, peroxisome proliferator-activated receptor alpha, and nuclear factor erythroid 2-related factor 2. Drug Metab Dispos **2009**;37(4):847-56.

64. Yueh MF, Tukey RH. Nrf2-Keap1 signaling pathway regulates

human UGT1A1 expression in vitro and in transgenic UGT1 mice. J Biol Chem **2007**;282(12):8749-58.

65. Berent AC, Tobias KM. Portosystemic vascular anomalies. Vet Clin North Am Small Anim Pract **2009**;39(3):513-41.
66. Hanahan D, Weinberg RA. Hallmarks of cancer: the next generation. Cell **2011**;144(5):646-74.
67. Fausto N. Mouse liver tumorigenesis: models, mechanisms, and relevance to human disease. Semin Liver Dis **1999**;19(3):243-52.
68. Maeda S, Kamata H, Luo JL, Leffert H, Karin M. IKKbeta couples hepatocyte death to cytokine-driven compensatory proliferation that promotes chemical hepatocarcinogenesis. Cell **2005**;121(7):977-90.
69. Patra KC, Hay N. The pentose phosphate pathway and cancer. Trends Biochem Sci **2014**;39(8):347-54.
70. Wang C, Guo K, Gao D, Kang X, Jiang K, Li Y, *et al.* Identification of transaldolase as a novel serum biomarker for hepatocellular carcinoma metastasis using xenografted mouse model and clinic samples. Cancer Lett **2011**;313(2):154-66.
71. Xu IM, Lai RK, Lin SH, Tse AP, Chiu DK, Koh HY, *et al.* Transketolase counteracts oxidative stress to drive cancer development. Proc Natl Acad Sci U S A **2016**;113(6):E725-34.
72. Mitsuishi Y, Taguchi K, Kawatani Y, Shibata T, Nukiwa T, Aburatani H, *et al.* Nrf2 redirects glucose and glutamine into anabolic pathways in metabolic reprogramming. Cancer Cell **2012**;22(1):66-79.

73. Sporn MB, Liby KT. NRF2 and cancer: the good, the bad and the importance of context. Nat Rev Cancer **2012**;12(8):564-71.
74. Khor TO, Huang MT, Prawan A, Liu Y, Hao X, Yu S, *et al.* Increased susceptibility of Nrf2 knockout mice to colitis-associated colorectal cancer. Cancer Prev Res (Phila) **2008**;1(3):187-91.
75. Xu C, Huang MT, Shen G, Yuan X, Lin W, Khor TO, *et al.* Inhibition of 7,12-dimethylbenz(a)anthracene-induced skin tumorigenesis in C57BL/6 mice by sulforaphane is mediated by nuclear factor E2-related factor 2. Cancer Res **2006**;66(16):8293-6.
76. Satoh H, Moriguchi T, Takai J, Ebina M, Yamamoto M. Nrf2 prevents initiation but accelerates progression through the Kras signaling pathway during lung carcinogenesis. Cancer Res **2013**;73(13):4158-68.
77. Rolfs F, Huber M, Kuehne A, Kramer S, Haertel E, Muzumdar S, *et al.* Nrf2 Activation Promotes Keratinocyte Survival during Early Skin Carcinogenesis via Metabolic Alterations. Cancer Res **2015**;75(22):4817-29.
78. DeNicola GM, Karreth FA, Humpton TJ, Gopinathan A, Wei C, Frese K, *et al.* Oncogene-induced Nrf2 transcription promotes ROS detoxification and tumorigenesis. Nature **2011**;475(7354):106-9.
79. Trachootham D, Alexandre J, Huang P. Targeting cancer cells by ROS-mediated mechanisms: a radical therapeutic approach? Nat Rev Drug Discov **2009**;8(7):579-91.
80. Skoko JJ, Wakabayashi N, Noda K, Kimura S, Tobita K,

Shigemura N, *et al.* Loss of Nrf2 in mice evokes a congenital intrahepatic shunt that alters hepatic oxygen and protein expression gradients and toxicity. Toxicol Sci **2014**;141(1):112-9.

81. Heindryckx F, Colle I, Van Vlierberghe H. Experimental mouse models for hepatocellular carcinoma research. Int J Exp Pathol **2009**;90(4):367-86.
82. Cairns RA, Harris IS, Mak TW. Regulation of cancer cell metabolism. Nat Rev Cancer **2011**;11(2):85-95.
83. Gorrini C, Harris IS, Mak TW. Modulation of oxidative stress as an anticancer strategy. Nat Rev Drug Discov **2013**;12(12):931-47.
84. Shibata T, Kokubu A, Saito S, Narisawa-Saito M, Sasaki H, Aoyagi K, *et al.* NRF2 mutation confers malignant potential and resistance to chemoradiation therapy in advanced esophageal squamous cancer. Neoplasia **2011**;13(9):864-73.
85. Dow LE, O'Rourke KP, Simon J, Tschaharganeh DF, van Es JH, Clevers H, *et al.* Apc Restoration Promotes Cellular Differentiation and Reestablishes Crypt Homeostasis in Colorectal Cancer. Cell **2015**;161(7):1539-52.
86. Burrell RA, McGranahan N, Bartek J, Swanton C. The causes and consequences of genetic heterogeneity in cancer evolution. Nature **2013**;501(7467):338-45.
87. Alizadeh AA, Aranda V, Bardelli A, Blanpain C, Bock C, Borowski C, *et al.* Toward understanding and exploiting tumor heterogeneity. Nat Med **2015**;21(8):846-53.

88. Bedard PL, Hansen AR, Ratain MJ, Siu LL. Tumour heterogeneity in the clinic. Nature **2013**;501(7467):355-64.
89. Collins FS, Varmus H. A new initiative on precision medicine. N Engl J Med **2015**;372(9):793-5.
90. Vargas AJ, Harris CC. Biomarker development in the precision medicine era: lung cancer as a case study. Nat Rev Cancer **2016**;16(8):525-37.
91. Friedman AA, Letai A, Fisher DE, Flaherty KT. Precision medicine for cancer with next-generation functional diagnostics. Nat Rev Cancer **2015**;15(12):747-56.
92. Collins DC, Sundar R, Lim JS, Yap TA. Towards Precision Medicine in the Clinic: From Biomarker Discovery to Novel Therapeutics. Trends Pharmacol Sci **2017**;38(1):25-40.
93. Lyman GH, Moses HL. Biomarker Tests for Molecularly Targeted Therapies--The Key to Unlocking Precision Medicine. N Engl J Med **2016**;375(1):4-6.
94. Park JY, Kricka LJ, Fortina P. Next-generation sequencing in the clinic. Nat Biotechnol **2013**;31(11):990-2.
95. Goodwin S, McPherson JD, McCombie WR. Coming of age: ten years of next-generation sequencing technologies. Nat Rev Genet **2016**;17(6):333-51.
96. Gawad C, Koh W, Quake SR. Single-cell genome sequencing: current state of the science. Nat Rev Genet **2016**;17(3):175-88.
97. Zhang X, Marjani SL, Hu Z, Weissman SM, Pan X, Wu S. Single-Cell Sequencing for Precise Cancer Research: Progress and Prospects. Cancer Res **2016**;76(6):1305-12.

98. Navin NE. The first five years of single-cell cancer genomics and beyond. Genome Res **2015**;25(10):1499-507.
99. Navin NE. Delineating cancer evolution with single-cell sequencing. Sci Transl Med **2015**;7(296):296fs29.
100. Shaw JA, Guttery DS, Hills A, Fernandez-Garcia D, Page K, Rosales BM, *et al.* Mutation Analysis of Cell-Free DNA and Single Circulating Tumor Cells in Metastatic Breast Cancer Patients with High Circulating Tumor Cell Counts. Clin Cancer Res **2017**;23(1):88-96.
101. Crowley E, Di Nicolantonio F, Loupakis F, Bardelli A. Liquid biopsy: monitoring cancer-genetics in the blood. Nat Rev Clin Oncol **2013**;10(8):472-84.
102. Dawson SJ, Tsui DW, Murtaza M, Biggs H, Rueda OM, Chin SF, *et al.* Analysis of circulating tumor DNA to monitor metastatic breast cancer. N Engl J Med **2013**;368(13):1199-209.
103. Thierry AR, Mouliere F, El Messaoudi S, Mollevi C, Lopez-Crapez E, Rolet F, *et al.* Clinical validation of the detection of KRAS and BRAF mutations from circulating tumor DNA. Nat Med **2014**;20(4):430-5.
104. Newman AM, Bratman SV, To J, Wynne JF, Eclov NC, Modlin LA, *et al.* An ultrasensitive method for quantitating circulating tumor DNA with broad patient coverage. Nat Med **2014**;20(5):548-54.
105. Alix-Panabieres C, Pantel K. Clinical Applications of Circulating Tumor Cells and Circulating Tumor DNA as Liquid Biopsy. Cancer Discov **2016**;6(5):479-91.

106. Bettegowda C, Sausen M, Leary RJ, Kinde I, Wang Y, Agrawal N, *et al.* Detection of circulating tumor DNA in early- and late-stage human malignancies. Sci Transl Med **2014**;6(224):224ra24.
107. Alix-Panabieres C, Pantel K. Real-time liquid biopsy: circulating tumor cells versus circulating tumor DNA. Ann Transl Med **2013**;1(2):18.
108. Menegon S, Columbano A, Giordano S. The Dual Roles of NRF2 in Cancer. Trends Mol Med **2016**;22(7):578-93.
109. No JH, Kim YB, Song YS. Targeting nrf2 signaling to combat chemoresistance. J Cancer Prev **2014**;19(2):111-7.
110. Kay MA. State-of-the-art gene-based therapies: the road ahead. Nat Rev Genet **2011**;12(5):316-28.
111. Zuckerman JE, Davis ME. Clinical experiences with systemically administered siRNA-based therapeutics in cancer. Nat Rev Drug Discov **2015**;14(12):843-56.
112. Wittrup A, Lieberman J. Knocking down disease: a progress report on siRNA therapeutics. Nat Rev Genet **2015**;16(9):543-52.
113. Jackson AL, Linsley PS. Recognizing and avoiding siRNA off-target effects for target identification and therapeutic application. Nat Rev Drug Discov **2010**;9(1):57-67.
114. Fellmann C, Gowen BG, Lin PC, Doudna JA, Corn JE. Cornerstones of CRISPR-Cas in drug discovery and therapy. Nat Rev Drug Discov **2017**;16(2):89-100.
115. Dominguez AA, Lim WA, Qi LS. Beyond editing: repurposing CRISPR-Cas9 for precision genome regulation and

interrogation. Nat Rev Mol Cell Biol **2016**;17(1):5-15.

116. Cox DB, Platt RJ, Zhang F. Therapeutic genome editing: prospects and challenges. Nat Med **2015**;21(2):121-31.

117. McGranahan N, Swanton C. Biological and therapeutic impact of intratumor heterogeneity in cancer evolution. Cancer Cell **2015**;27(1):15-26.

118. Totoki Y, Tatsuno K, Covington KR, Ueda H, Creighton CJ, Kato M, *et al.* Trans-ancestry mutational landscape of hepatocellular carcinoma genomes. Nat Genet **2014**;46(12):1267-73.

119. Comprehensive molecular profiling of lung adenocarcinoma. Nature **2014**;511(7511):543-50.

120. Riaz N, Morris LG, Lee W, Chan TA. Unraveling the molecular genetics of head and neck cancer through genome-wide approaches. Genes Dis **2014**;1(1):75-86.

121. Boj SF, Hwang CI, Baker LA, Chio, II, Engle DD, Corbo V, *et al.* Organoid models of human and mouse ductal pancreatic cancer. Cell **2015**;160(1-2):324-38.

122. Fatehullah A, Tan SH, Barker N. Organoids as an in vitro model of human development and disease. Nat Cell Biol **2016**;18(3):246-54.

123. Yu M, Bardia A, Aceto N, Bersani F, Madden MW, Donaldson MC, *et al.* Cancer therapy. Ex vivo culture of circulating breast tumor cells for individualized testing of drug susceptibility. Science **2014**;345(6193):216-20.

124. Goldstein LD, Lee J, Gnad F, Klijn C, Schaub A, Reeder J, *et al.*

Recurrent Loss of NFE2L2 Exon 2 Is a Mechanism for Nrf2 Pathway Activation in Human Cancers. Cell Rep **2016**;16(10):2605-17.

Table 1: The sequences of primers used for genotyping

Gene symbol	Primer name	Primer sequence
Nrf2 WT	g*Nrf2*-F:	5'-GGA ATG GAA AAT AGC TCC TGC C-3'
	g*Nrf2*-R:	5'-GCC TGA GAG CTG TAG GCC C-3'
Nrf2 KO	g*Nrf2*-R':	5'-GGG TTT TCC CAG TCA CGA C-3'
ARE-hPAP	ARE-hPAP-F:	5'-CTA GAG TCA CAG TGA CTT GGC AAA-3'
	ARE-hPAP-R:	5'-GGA AGA TGA TGA GGT TCT TGG CGG-3'

1*

* F: Forward
R: Reverse
g: genomic
h: human
m: murine

Table 2: The sequences of primers used for qPCR

Gene symbol	Primer name	Primer sequence
Gapdh	m *Gapdh* -F	5'-GCC CTT GAG CTA GGA CTG G-3'
	m *Gapdh* -R	5'-GGG CTG CAG TCC GTA TTT AT-3'
Nqo1	m *Nqo1*-F	5'-GGC CCA TTC AGA GAA GAC AT-3'
	m *Nqo1*-R	5'-TTC GAG TAC CTC CCA TCC TC-3'
Hmox1	m *Hmox1*-F	5'-CCA CTC CCT GTG TTT CCT TT-3'
	m *Hmox1*-R	5'-GCT GCT GGT TTC AAA GTT CA-3'
Gclc	m *Gclc*-F	5'-GCA GCA TAT CTG AGG CAA GA-3'
	m *Gclc*-R	5'-CTG ACA CGT AGC CTC GGT AA-3'
Glut1	m *Glut1*-F	5'-GCT GCC AGG TTC TAG TCT CC-3'
	m *Glut1*-R	5'-AGT GTC CGT GTC TTC AGC AG-3'
G6pdx	m *G6pdx* -F	5'-AGG AAG TGG TCA AGG ACA CC-3'
	m *G6pdx* -R	5'-TAT TGC TAG GCA GCA TGA GG-3'
Pgd	m *Pgd*-F	5'-CGT AAG GCC CTC TAT GCT TC-3'
	m *Pgd*-R	5'-GGA ACA CAC TTC GGA TGA TG-3'
Taldo	m *Taldo*-F	5'-CAG ACC AGT GAC TCG GAG AA-3'
	m *Taldo*-R	5'-AGC ATC CGC TCC AAC TTT AT-3'
Tkt	m *Tkt*-F	5'- TAT GGG TGG TCA CTG CTG TT-3'
	m *Tkt*-R	5'-GCT AGC TGA GCA GTT TGT CG-3'

Me1	m *Me1*-F	5’-GCA TGC CAG CAG TAC AGT TT-3’
	m *Me1*-R	5’-GAT GCG CTC TCC ATC AGT TA-3’
Idh1	m *Idh1* -F	5’-AAG CTA TGA AGT CCG AGG GA-3’
	m *Idh1*-R	5’- CCA TCT GGA CAA ATC AGC AC-3’
Ppat	m *Ppat*-F	5’- ATG GAA ATC GTC CTC TCT GC-3’
	m *Ppat*-R	5’-CCA CCC ATC CTT CAG TTT CT-3’
Mthfd2	m *Mthfd2*-F	5’-CGG CAC TCC CTT ACT CTC TC-3’
	m *Mthfd2*-R	5’-GGG AGA CTC TAA CCC TTC CC-3’

Table 3: The primers used for identifying mutations in *Nrf2*

Gene symbol	Primer name	Primer sequence
Nrf2	m g*Nrf2*-F	5’-CTC ACA AAG TCC TCC CTG TGA T-3’
	m g*Nrf2*-R	5’-TTG AGT GAA TGG AAT TGA CAG TCT T-3’

Table 4: The sequences of primers used for constructing plasmids and site-directed mutagenesis study

Gene symbol	Primer name	Primer sequence
Nrf2	m *Nrf2*-D29G-F	5’-TGG AGG CAA GAC ATA GGT CTT GGA GTA AGT CGA-3’
	m *Nrf2*-D29G-R	5’-TCG ACT TAC TCC AAG ACC TAT GTC TTG CCT CCA-3’
	m *Nrf2*-V32E-F	5’-GAC ATA GAT CTT GGA GAA AGT CGA GAA GTG TTT-3’
	m *Nrf2*-V32E-R	5’-AAA CAC TTC TCG ACT TTC TCC AAG ATC TAT GTC-3’
	m *Nrf2*-T80A-F	5’-CAA CTG GAT GAA GAA GCA GGA GAA TTC CTC CCA-3’
	m *Nrf2*-T80A-R	5’-TGG GAG GAA TTC TCC TGC TTC TTC ATC CAG TTG-3’
	m *Nrf2*- stop codon-F	5’-ATG ATG GAC TTG GAG TAG CCA

Nrf2		CCG CCA GGA CTA-3’
	m *Nrf2* stop codon-R	5’-TAG TCC TGG CGG TGG CTA CTC CAA GTC CAT CAT-3’
	h *NRF2*-D29G-F	5’-TGG AGG CAA GAT ATA GGT CTT GGA GTA AGT CGA-3’
	h *NRF2*-D29G-R	5’-TCG ACT TAC TCC AAG ACC TAT ATC TTG CCT CCA-3’
	h *NRF2*-T80P-F	5’-CAA CTA GAT GAA GAG CCA GGT GAA TTT CTC CCA-3’
	h *NRF2*-T80P-R	5’-TGG GAG AAA TTC ACC TGG CTC TTC ATC TAG TTG-3’

	Kaplan-Meier Analysis		
	From TCGA		
	Cases with Alterations in *Nrf2*		
No#	Case ID	Time (months)	Types of *Nrf2* Mutation
#1	TCGA-FV-A496	0.33	Nrf2 amplification
#2	TCGA-DD-AAC8	0.53	E82G
#3	TCGA-T1-A6J8	0.76	Nrf2 amplification
#4	TCGA-5R-AAAM	1.51	T80I
#5	TCGA-G3-AAV6	2.14	Nrf2 amplification
#6	TCGA-DD-A1EE	11.47	I28del
#7	TCGA-G3-AAV3	13.53	G81A
#8	TCGA-DD-A1EL	13.63	Nrf2 amplification
#9	TCGA-DD-AACQ	14.19	Nrf2 amplification
#10	TCGA-RC-A7SK	15.51	Nrf2 amplification
#11	TCGA-BC-A8YO	18.46	Nrf2 amplification
#12	TCGA-EP-A2KA	20.6	Nrf2 amplification
#13	TCGA-DD-A39V	21.12	E82D
#15	TCGA-DD-AAEH	25.76	D27Y
#16	TCGA-DD-A4NI	26.81	Q26P
#17	TCGA-BC-A10T	27.5	Nrf2 amplification
#18	TCGA-KR-A7K8	29.76	Nrf2 amplification
#19	TCGA-DD-AADJ	35.02	G81C
#20	TCGA-DD-AAVS	59.89	I28M, Q26R
#21	TCGA-DD-AAVY	64.72	G81R
#22	TCGA-DD-AAVU	72.34	Q61H
#23	TCGA-DD-A4NO	73.75	E79V, E79*
	From AMC		
	Cases with Alterations in *Nrf2*		
No#	Case ID	Time (months)	Types of *Nrf2* Mutation
#1	H050510	6.9	G81S
#2	H060098	26.3	T80A
#3	H093295	27.5	Q26H
#4	H072511	35.6	L30P
#5	H093904	37.7	D16E
#6	H080025	60.7	E82A

Dataset S1. HCC patients with *Nrf2* mutations. Abbreviations: TCGA, The Cancer Genome Atlas; AMC, Asan Medical Center.

ABSTRACT IN KOREAN (국문초록)

Diethylnitrosamine 으로 유도된 간암 발생과정 에서 Nrf2 의 역할

암으로 인한 사망 중 가장 큰 원인인 간암은 표현형 혹은 유전적으로 서로 다른 형질 (heterogeneous)을 갖는 것으로 알려져 있다. Nrf2는 세포내 다양한 스트레스에 의해 활성화 되어 항산화, 해독화 효소들의 발현을 촉진시키는 전사인자로 생체내 방어 기전에 관여하며 간암의 화학적 암예방의 주요한 표적 단백질로 보고되고 있다. 그러나 Nrf2 결핍마우스에 cytochrome p450 2E1 (Cyp2e1)에 의한 DEN의 대사적 활성화의 약화나 간의 혈관구조 (hepatic vasculature)의 손상 없이 diethylnitrosamine (DEN)에 의해 유도되는 간암 발생에 있어서 저항기전을 보여 오히려 암화를 촉진시켰다. 본 연구에서는 DEN에 의해 유도되는 간암 발생 기전에 있어서 Nrf2의 역할과, Nrf2의 활성이 어떻게 조절 될 수 있는지 알아보고자 하였다. 간의 종양에서 Nrf2의 단백질의 발현과 핵내 이동, Nrf2의 전사적 활성이 증가되어 있으며, DEN에 의해 유도되는 Nrf2의 과발현이 간암세포의 성장속도를 증가시켰다. 그 분자적 기전

을 살펴본 결과 DEN 처리시 Nrf2의 유전자 파열/파괴 (genetic disruption)이 글루코오스 흡수 (glucose uptake)와 펜토오스 인산 경로 (pentose phosphate pathway)에 관여하는 효소들의 운반체 (transporter)의 발현을 감소시킴으로 간암으로의 진행이 약화되었다. 또한 세포내 잘 알려진 Nrf2 억제 단백질인 Keap1과의 결합 도메인의 변형(alteration)이 Nrf2의 과도한 활성화 현상을 야기시켰으며, Nrf2의 활성화된 돌연변이주를 지닌 간암 환자는 그렇지 않은 환자에 비해 전체 생존기간 (overall survival)이 짧음을 확인 할 수 있었다. 결론적으로 Nrf2는 간암발생을 촉진시키며 향후 항암제 치료의 목표물로 기능할 수 있음을 제시 할 수 있다.

Keywords: Nrf2, diethylnitrosamine, hepatocarcinogenesis, antioxidant response elements, pentose phosphate pathway.

Student Number: 2013-31345